NTNU – Trondheim
Norwegian University of
Science and Technology

Cellular Effects of Insulin in Human THP-1 Monocytes

Jamal Naderi

Biotechnology
Submission date: Januar 2015
Supervisor: Berit Johansen, IBI
Co-supervisor: Astrid Jullumstrø Feuerherm, IBI
Thuy Nguyen, IBI

Norwegian University of Science and Technology
Department of Biology

NTNU – Trondheim
Norwegian University of
Science and Technology

Cellular Effects of Insulin in Human THP-1 Monocytes

Jamal Naderi

Biotechnology (MSc)

Submission date: January 2015

Supervisor: Prof. Berit Johansen

Co-supervisors: Post-Doc. Astrid Jullumstrø Feuerherm

Dr. Thanh Thuy Thi Nguyen

Norwegian University of Science and Technology

Department of Biology

“Knowing is not enough; we must apply. Willing is not enough; we must do.”

-Johann Wolfgang Von Goethe

Abstract

Excess of insulin in the circulating blood relative to the level of glucose (Hyperinsulinemia) may be linked to systemic low-grade inflammation and some chronic disease such as the metabolic syndrome, type 2 diabetes (T2D), and cardiovascular disease (CVD). The function of high levels of insulin in vascular smooth muscle cells (VSMCs), endothelial cells (ECs), and macrophages in relation to CVD has been investigated, but exact role of high insulin levels in monocytes, as an important cell type in the pathogenesis of CVD, is largely unknown. In order to better understand the physiological consequences of high levels of insulin in monocytes, we investigated the cellular effects of insulin in THP-1 human monocytic cell line by cell counting, resazurin assay, and flow cytometry cell cycle phase analysis in a dose- and time-dependent manner.

We found that insulin induces dose- and time-dependent hyperproliferation of THP-1 cells, as observed by cell counting (significant and most evident increase in cell numbers by 23 % following 24 h at 100 nM insulin). Insulin did not change THP-1 monocytic morphology and color of culture medium, as monitored by microscopy. Insulin treatment also did not trigger cell adhesion to the bottom of culture flasks or clustering of cells. These findings are in agreement with a hyperproliferative effect of insulin in THP-1 monocytes as observations suggest that insulin may not promote differentiation of monocytes to macrophages. Insulin increases metabolic activity of monocytes in a cell density-, time- and dose-dependent fashion (significant increase in metabolic activity following 24 h with a seeding density of 20000

cells/well at 20 nM and 100 nM insulin, each by 5 %), as shown by resazurin bioassays. These stimulatory effects of insulin on cell proliferation and metabolic activity subsided following longer exposure periods. Finally, by flow cytometry, we demonstrated that insulin alters cell cycle phase distribution supporting that insulin may indeed be a dose- and time-dependent inducer of mitosis (significant and most evident alteration following 24 h at 100 nM insulin), hence this result validates the findings by cell counting and resazurin assay in favor of increased proliferation by insulin.

In conclusion, the results of this study suggest that insulin increases monocyte proliferation, and hence may affect important aspects of monocyte function, for instance immune and vascular function.

Acknowledgements

This master's thesis was conducted at the Norwegian University of Science and Technology at the Faculty of Natural Science and Technology; Department of Biology in the period January 2013 until January 2015. The head supervisor was Professor Berit Johansen, and the co-supervisors were senior researcher Dr. Astrid Jullumstrø Feuerherm and Dr. Thanh Thuy Thi Nguyen.

I would like to express my heartfelt gratitude to Astrid. Thank you so much for your constructive feedback, being positive and generous with your time. Thuy, thank you for valuable training at the cell culture laboratory. Last but not least, I would like to thank Berit for excellent advice when needed and always being available.

Trondheim, January 2015

Jamal Naderi

List of abbreviations

AMPK	Adenosine monophosphate-activated protein kinase
ApN	Adiponectin
BrdU	Bromodeoxyuridine
CD14	Cluster of differentiation 14
CD16	Cluster of differentiation 16
CNS	Central nervous system
COX-2	Cyclooxygenase-2.
CVD	Cardiovascular disease
DC	Dendritic cell
DMSO	Dimethyl sulfoxide
DNA	Deoxyribonucleic acid
EC	Endothelial cell
ECM	Extracellular matrix
ERK	Extracellular-signal regulated kinase
FBS	Fetal bovine serum
FL3	Fluorescent channel3

FS	Forward scatter
GLUT4	Glucose transporter 4
HCAEC	Human coronary artery endothelial cell
HCSMC	Human coronary smooth muscle cell
HDL	High-density lipoprotein
HGP	Hepatic glucose production
IGF-1	Insulin-like growth factor-1
IGF-1R	Insulin-like growth factor-1 receptor
IKK	IκB kinase
IL	Interleukin
INS	Insulin
IR	Insulin receptors
IRS	Insulin receptor substrates
JNK	c-jun N-terminal kinase
LBP	LPS-binding protein
LPS	Lipopolysaccharide
MAPK	Mitogen-activated protein kinase

SD	Standard deviation
MMP-9	Matrix metalloproteinase-9
MCP-1	Monocyte chemoattractant protein-1
MQ water	Milli-Q water
mTOR	Mammalian target of rapamycin
NADH	Nicotinamide adenine dinucleotide
OD	Optical density
$p70^{rsk}$	p70 ribosomal S6 kinase
PAI-1	Plasminogen activator inhibitor-1
PBS	Phosphate buffered saline
PDK1	3-Phosphoinositide-dependent protein kinase 1
PI	Propidium iodide
PI3K	Phosphoinositide 3-kinase
RNA	Ribonucleic acid
SH2	Srchomology-2
SMC	Smooth muscle cell
SPF	S-phase fraction

T25	25 cm^2 tissue culture flask
T2D	Type 2 diabetes
TNF-α	Tumor necrosis factor-α
tPA	Tissue-type plasminogen activator
uPA	Urokinase-type plasminogen activator
VEGF	Vascular endothelial growth factor
VSMC	Vascular smooth muscle cell
WAT	White adipose tissue

Table of Content

1. INTRODUCTION

1.1 Insulin and metabolic processes

Insulin is a peptide hormone that regulates metabolism of glucose, lipid, and protein. The hormone also controls gene expression and activities of some metabolic enzymes. All these insulin's effects are performed by a complex network of signaling pathways (Figure 1). Based on information thereof, insulin acts as a vital hormone in mammals [1], and defect(s) in cellular processes coordinated by insulin signaling could have severe consequences.

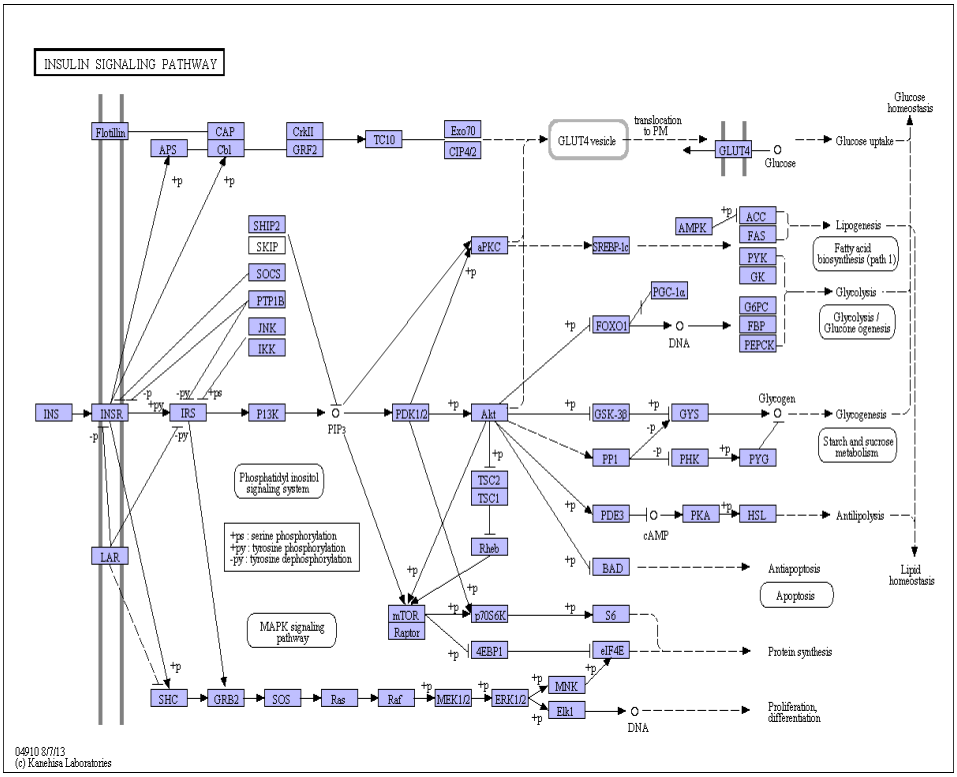

Figure 1 Complex network of signaling pathways in response to insulin. Insulin binds to its receptor that induces the tyrosine phosphorylation of IRS. IRSs activate the regulatory subunit of PI3K, and PI3K results in activation of PDK1, which activates Akt. Akt has a key role in metabolism. INS, insulin; INSR, insulin receptor; IRS, insulin receptor substrates; PI3K, phosphoinositide 3-kinase; PDK1, 3-phosphoinositide-dependent protein kinase 1; JNK, JUN N-terminal kinase; IKK, IκB kinase; mTOR, mammalian target of rapamycin; ERK, extracellular signal-regulated kinase [2].

1.1.1 Insulin and the regulation of glucose metabolism

Consumption of diets high in glycemic carbohydrates causes postprandial hyperglycemia, which in turn induces the primary role of insulin; reducing blood glucose [3]. The concentrations of insulin after a meal in normal and insulin-resistant individuals are ~0.3- 0.4 nM and ~1.4- 1.5 nM, respectively [4].

Under normal conditions, insulin is secreted from the β-cells of the islets of Langerhans in the pancreas in response to an escalation in blood glucose levels. Insulin then suppresses hepatic glucose production (HGP) in the liver. The hormone stimulates glucose uptake, utilization, and storage in fat and muscle [5-8] by stimulating the translocation of the glucose transporter GLUT4 from intracellular sites to the plasma membrane of fat and muscle cells. Insulin promotes glycogen storage through a coordinated increase in glucose transport and glycogen synthesis [5]. Thus, the islet response returns elevated plasma glucose, for instance after a meal, to baseline [6].

In insulin resistance, a condition associated with dietary and/or genetic factors that causes obesity, glucose homeostasis is conserved by capacity of the islets of Langerhans to escalate insulin secretion in a compensatory way. If islet dysfunction prevents the increase of insulin secretion needed to overcome insulin resistance, glucose intolerance will arise. The progress of islet dysfunction involves increased HGP and reduced tissue

glucose uptake that eventually lead to overt hyperglycemia and diabetes [6].

1.2 Insulin resistance

Insulin resistance is defined as a condition where target tissues, such as the skeletal muscle, liver, and adipocytes, decrease the response to insulin [9, 10]. The insulin resistance is characterized by defect at many steps, with reduction in receptor concentration and kinase activity [11], IRS-1 and -2 concentration and phosphorylation, PI3K activity, translocation of glucose transporter, and intracellular enzymes activity [5]. Hyperinsulinemia per se may promote insulin resistance [12]. Genetic and acquired factors can affect insulin sensitivity. Genetic defects in the insulin receptor represent the most severe form of insulin resistance [5].

There is no evidence that insulin resistance addresses every tissue on which insulin has effects. The muscle and adipose tissue are the main tissues in which insulin resistance takes place [13]. The pathophysiology of type 2 diabetes (T2D) is caused by combination of insulin resistance in classic target tissues, such as liver, muscle, and fat, coupled with insulin resistance in β-cell, brain, and other tissues [5]. In addition, insulin resistance is known as a predictor of cardiovascular disease (CVD) [14].

1.2.1 Insulin resistance and inflammation

Insulin resistance is known as a chronic low-level inflammatory state. Hyperinsulinemia and insulin action may be associated with hypertension, low high-density lipoprotein (HDL) cholesterol, hypertriglyceridemia, abdominal obesity, and glucose intolerance, linking all these conditions (metabolic syndrome) to the development of CVD [15].

The similarities of insulin resistance with another inflammatory state, atherosclerosis, have been characterized. Insulin resistance and atherosclerosis show similar pathophysiological mechanisms, primarily due to the roles of the two crucial proinflammatory cytokines, TNF-α and IL-6 [15]. The metabolic inflammation caused by postprandial hyperinsulinemia is involved in the lifestyle disease development including obesity-associated metabolic disorders, T2D, and CVD [3].

1.3 Mitogenic action of insulin

Insulin induces cell growth and differentiation [5]. Insulin acts on tissues through different mechanisms. The functions of insulin in glucose homeostasis appear to be mediated by the classical insulin receptor while the functions of insulin on cell growth are mediated by insulin-like growth factor 1 (IGF-1) receptor. Thus, if one signaling pathway interacts with insulin resistance, the other may still be accessible [13]. Some studies have shown that insulin's effects on cell growth involve multiple

kinases [16, 17] including the mitogen-activated protein kinase (MAPK) extracellular signal-regulated kinase (ERK) [5] and PI3K. PI3K has a critical role in the metabolic and mitogenic actions of insulin and IGF-1 [5, 18-20] (Figure 2). Inhibitors of class Ia PI3K, or transfections with dominant negative constructs of the enzyme suppress most metabolic functions of insulin, including stimulation of glucose transport, glycogen, and lipid synthesis [5]. Insulin induces proliferation, such as VSMCs proliferation, through a mechanism involving the PI3K [19, 21].

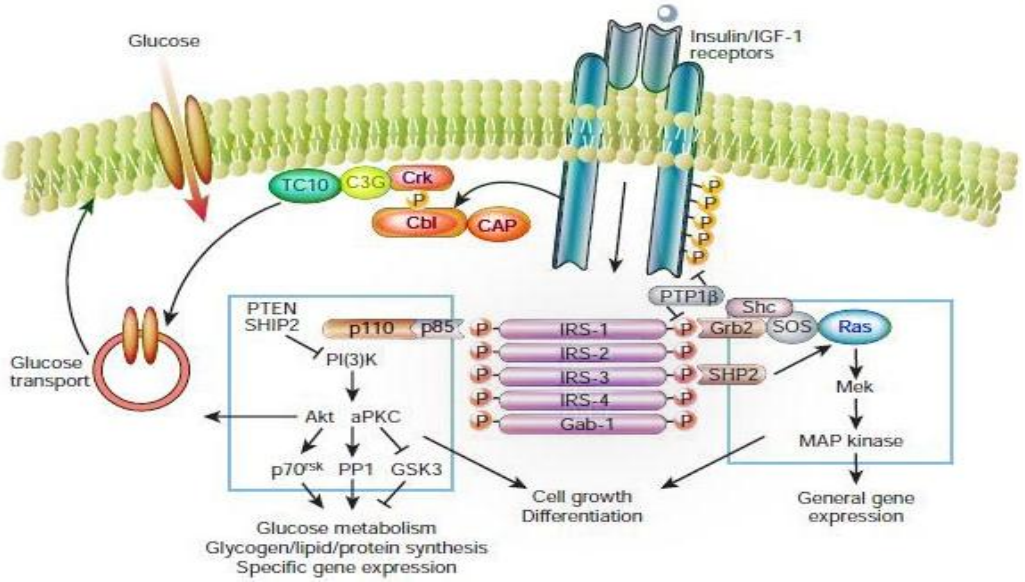

Figure 2 Signaling pathway in insulin action related to cell growth. The insulin receptor experiences autophosphorylation, and catalyses the phosphorylation of intracellular proteins such as members of the insulin receptor substrate (IRS) family, Shc, and CbI. Upon tyrosine phosphorylation, these proteins interact as docking sites with proteins that contain SH2 (Srchomology-2) domains [5, 22], culminating in a various series of signaling pathways, including activation of PI3K and downstream PtdIns(3,4,5)P_3-dependent protein kinases, Ras and the MAPK cascade, and CbI/CAP and the activation of TC10. IGF-1, insulin-like growth factor 1; $p70^{rsk}$, p70 ribosomal S6 kinase [5]. Modified figure [5].

It has been confirmed that metabolic and mitogenic insulin signaling pathways present distinct sensitivity to some common stimuli, are independently regulated, and may act on VSMCs migration, proliferation and inflammation in chronic hyperinsulinemia that indicate VSMCs are responsive to insulin [5, 23]. The inhibition of metabolic insulin signal increases insulin-stimulated proliferation of endothelial cells [24]. Hyperinsulinemia in association with increased levels of fatty acids may impair glucose homeostasis simultaneously with the overactivation of smooth muscle cell of arterial wall, proliferation and inflammation; these events could make arterial plaques [23].

1.4 Monocytes

Leukocyte subsets are distinguished by physical and functional characteristics. They originate from hematopoietic stem cells and evolve along distinct differentiation pathways in response to internal and external signals [25]. The mononuclear phagocyte system comprises a subcategory of leukocytes originally defined as a population of bone marrow-derived myeloid cells that circulate in blood as monocytes and populate tissues as macrophages in the steady state and during inflammation [25, 26]. Monocytes circulate in the bone marrow, blood, and spleen and do not proliferate in a steady state [25]. In other words, monocytes are deemed circulating, whereas macrophages and dendritic cells (DCs) are tissue resident and mainly sessile [27]. Based on levels of CD14 and CD16, monocytes can be divided into three types: classical

($CD14^{++}CD16^{-}$), non-classical ($CD14^{+}CD16^{++}$) and intermediate ($CD14^{++}CD16^{+}$) [26, 28-30]. CD14 is the most substantial endotoxin (LPS) receptor on monocytes and neutrophils involved in activation of these cells by LPS [31]. CD14 is a 55 kD polypeptide [32] which is linked to the membranes of differentiated myeloid cells [33]. LPS-binding protein (LBP), existing in the serum of healthy human beings, mediates and boosts the binding of LPS to CD14. The different cytokines and also LPS itself can alter the number of surface-expressed CD14 and the amount of released sCD14 on monocytes and neutrophils. There are diverse diseases that are accompanied by alterations of systemic or local sCD14 levels or CD14 expression on cells. High numbers and activation of $CD14^{++}$ monocyte subsets are linked to hyperglycemia and cardiovascular complications in obese patients [26]. These findings suggest that the expression of CD14 might be important in the regulation of the inflammatory process [31]. THP-1 monocytic cells are known to express CD14 (+) [31-35].

Monocytes are crucial immune cells in the blood [3], equipped with a wide variety of receptors [27] such as chemokine receptors and adhesion receptors that mediate migration from the blood to the tissue during infection. They generate inflammatory cytokines and take up toxic molecules and cells. They can also differentiate into inflammatory DCs or macrophages during inflammation and perhaps, less effectively, in the steady state. Migration of monocytes to tissues and differentiation to inflammatory DCs and macrophages are presumably regulated by the inflammatory milieu and pathogen-associated pattern-recognition receptors [25].

1.4.1 Postprandial monocyte activation and the risk of CVD

High-glycemic load diets (consumption of diets high in carbohydrate) have been implicated in obesity, insulin sensitivity, circulating lipid concentrations, endothelial function, and likely the risk of CVD [36]. There is a relation between high-glycemic load diets, high insulin levels, hyperlipidemia, and monocyte activation (production of cytokines), all significant risk factors for T2D and CVD [3, 36]. CVD may be triggered and progressed by inflammation events. Activation of immune cells such as monocytes triggers inflammation, an important process in CVD. Activation of circulating monocytes facilitates accumulation and sequestration of monocytes into the arterial intima, one of the early steps in plaque formation [36-39]. The production of cytokines including TNF-α and IL-1β (a hallmark of monocyte activation) activates the endothelium and causes augmented vascular permeability and expression of adhesion molecules, crucial events in CVD [36].

1.4.2 The human monocytic cell line THP-1 and cell growth

THP-1 is a human leukemia cell line derived from the blood of a boy suffering from acute monocytic leukemia. They are cultured *in vitro* as a suspension culture at 37℃ in the atmosphere of 5 % CO_2. Differentiation of monocytic THP-1 cells into macrophage-like cells is mainly performed using phorbol myristate acetate as this reagent triggers differentiation

[40-42]. THP-1 monocyte has a round shape, clear cytoplasm with a bean-shaped nucleus [43]. Figure 3 demonstrates THP-1 cells under a light microscope.

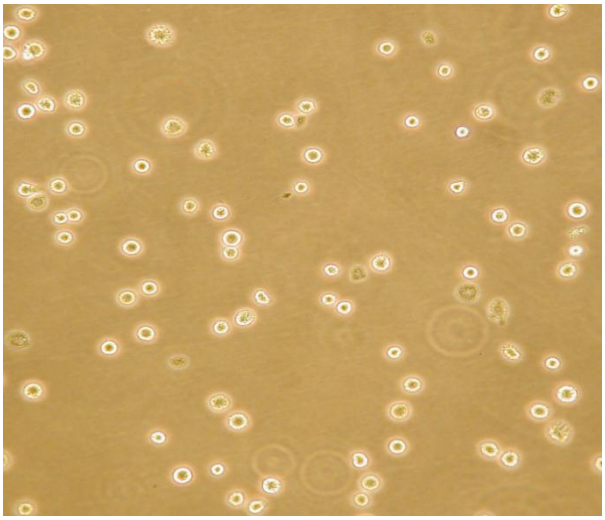

Figure 3 THP-1 monocytic cells growing in suspension (×20). [Credit: J. Naderi]

Since it is difficult to acquire large amounts of pure monocytes in human beings, the utilization of a human monocytic cell line such as THP-1 might provide a beneficial tool for studying monocytic leukemia and the function of monocytes, especially in the human immune response as THP-1 retains its monocytic properties and resembles the human monocyte [43]. In contrast to native human monocytes, the THP-1 cell line presents the extra asset of a homogeneous population, which distinctly facilitates further biochemical research [40, 44, 45]. The several studies reported that THP-1 is a suitable model-system for mimicking human monocytes and macrophages in metabolic inflammation, diabetes and vasculature-related research [46, 47].

The eukaryotic cell cycle is divided into four different phases (Figure 4): The G1- (first gap) phase is the preparation stage, where somatic cells grow in size and synthesise proteins and other components required for DNA synthesis. S- (synthesis) phase is the period where the cell replicates the chromosomes. G2- (second gap) is the period where the cell prepares for division. These three phases altogether are known as the interphase. The cell division, which consists of the division of the nucleus and then cytoplasm, happens in the M- (mitotic) phase; the M-phase is divided into several stages [48, 49].

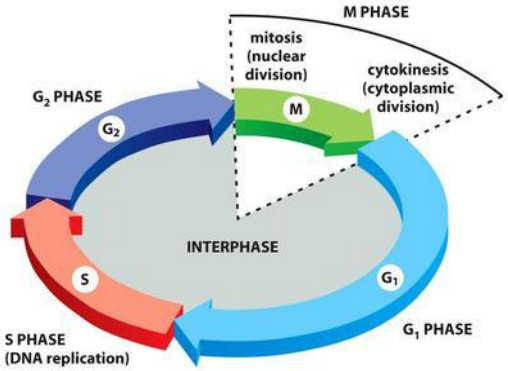

Figure 4 The cell cycle contains four different phases. G1-phase is the gap between M-phase and S-phase. DNA replication is limited to S-phase. G2-phase is the gap between S-phase and M-phase. These three phases altogether are known as the interphase. In M-phase, the nucleus and then the cytoplasm divide [49].

Cells in culture usually grow in a standard pattern of growth consisting of three phases: lag phase, log phase, and plateau phase. The lag phase is a period after subculturing cells where they adjust to the medium, with

little or no increase in cell number. In the log phase, cells are in exponential growth and most reproducible stage. In the plateau phase, cell growth is more or less equivalent to cell death, i.e. no net increase in cell numbers. Adhesive monolayer cells reach plateau phase, when they are in a very high density, due to contacting cells to each other. Suspension cells, like THP-1, do not demonstrate same plateau and saturated density, but will finally reach a plateau because of exhaustion of the medium [50].

Prior to experiments, it is recommended that cells should exist in log phase. Cells are randomly distributed in the cell cycle during log phase. Thus, cells should be synchronized prior to experiments [50]. This process can be attained through serum starvation of cells that may cause cells to enter the G_0-phase, referred to "out of cycle" [51].

1.5 Chronic high insulin levels, Obesity, T2D and CVD; a strong-hypothesized connection

The glycemic index (the rate of carbohydrate absorption after a meal) significantly affects postprandial hormonal and metabolic responses. High-glycemic index meals cause an initial period of high blood glucose and insulin levels, followed in many human beings by reactive hypoglycemia, counterregulatory hormone secretion, and increased concentrations of serum free fatty acid. This situation may contribute to excessive food intake, β-cell dysfunction, dyslipidemia, and endothelial dysfunction. Thus, the diet high in glycemic index may elevate the risk for obesity, T2D, and CVD, a hypothesis that elicits hefty support from studies [52].

Monocytes, macrophages, and lymphocytes are known as mononuclear cells (MNCs). MNCs proliferation and accumulation account for inflammation in both obesity/hyperinsulinemia and atherosclerosis. In obesity-associated hyperinsulinemia/insulin-resistant patients, the elevated concentrations of several inflammatory mediators (e.g. TNF-α, IL-6, monocyte chemoattractant protein-1 (MCP)-1, and matrix metalloproteinase-9 (MMP-9; gelatinase B)) likely promote MNC infiltration of adipose tissue and the vessel wall. Susceptible atherosclerotic lesions are characterized by elevated numbers of MNCs, potentially promoting plaque rupture through their excess levels of MMP-9 expression [53].

1.6 Aims of the thesis

The escalated incidence of obesity, insulin resistance, T2D, CVD, and other metabolic diseases in the western world calls for a better understanding of the mechanisms underlying these disorders and the outcomes thereof [54-57].

Insulin serves as the primary regulator of blood glucose concentration [5, 6] and is an essential hormone for metabolic homeostasis in mammals [1]. Insulin also stimulates cell growth and differentiation [5]. Hyperinsulinemia may stimulate various proliferative events e.g. in VSMCs [24] and ECs [58]. Insulin resistance as well as hyperinsulinemia, linked to T2D, promotes largely the progression of hypertension and atherosclerotic lesions [19]**.** Obesity-associated insulin resistance thrives in the existence of activated inflammatory signaling in liver, white adipose tissue (WAT), skeletal muscle, and even in the central nervous system (CNS) [59].

Monocytes may have a role in the risk of CVD [53]. Role of insulin in monocytes, linked with hyperinsulinemia and lifestyle diseases development, is largely unknown. This justifies a further research on characteristic of cellular effects of insulin on monocytes; this master's thesis investigates cellular effect of insulin on THP-1 monocytic proliferation, which might be pivotal in monocyte function, for instance, immune and vascular function in atherosclerotic process and/or CVD. In these areas of metabolic research, some questions remain unanswered that we aim to elucidate them in the present study:

Could the human THP-1 monocytic cell line be employed as a suitable model-system to study the effect of high levels of insulin at the cellular level?

Would THP-1 monocytes respond to increased level of insulin *in vitro*?

Will high insulin levels affect proliferation of monocytes *in vitro*?

May high levels of human insulin affect immune and vascular function?

2. MATERIALS AND METHODS

2.1 Reagents and solutions

The reagents and solutions, which were used in this study, are listed in Table 1.

Reagents and solutions	**Company**	**Catalog no.**
RPMI 1640-medium	Sigma-Aldrich	R0883
Fetal Bovine Serum (FBS)	Gibco	10270
Gentamicin solution	Sigma-Aldrich	G1397
L-Glutamine	Sigma-Aldrich	G5792
β-Mercaptoethanol	Sigma-Aldrich	M6250
Milli-Q (MQ) water	Millipore Corporate	N/A
Resazurin	R&D Systems	AR002
Insulin solution human	Sigma-Aldrich	I9278
Phosphate buffered saline (PBS)	Oxoid	BR0014G
RNase	Sigma-Aldrich	R6513
Methanol	Merck	1.06009.1000
Trypan Blue	Sigma-Aldrich	T8154
Propidium Iodide (PI)	Sigma-Aldrich	P4864

Table 1 Reagents and solutions.

2.2 Cell culture

2.2.1 Cell cultivation

The experiments were performed on human monocytic cell line THP-1 (American Type Culture Collection, Manassas, VA, Catalog No. TIB-202). THP-1 cells were maintained in suspension for passage and growth in RPMI-1640 supplemented with 10% heat-inactivated fetal bovine serum (FBS), 1% L-glutamine, 0.002% gentamicin, and 0.05 mM β-mercaptoethanol [3, 43]; the suspension cells were incubated at 37 ℃ in a humidified 5% CO_2 incubator.

2.2.2 Thawing of cells

Monocytic THP-1 cells, in CryoTubes, were taken from the liquid N_2 tank and immediately thawed in lukewarm water (37°C). To avoid explosive pressure inside of the CryoTube, its screw cap was loosened slightly before holding it in the water bath, carefully avoiding water to enter the vial. When the content of CryoTube became slush, its cap was tightened. The cells were transferred to a 15 ml tube using a transfer pipette, and 10 ml pre-warmed (37 ℃) growth medium was added very carefully (drop by drop), to avoid a rapid osmotic change and reduction of cell viability [50]. THP-1 suspension cells were centrifuged at 700 rpm at 25 ℃ for 5 minutes, and the supernatant (DMSO and medium) was discarded. DMSO is applied for freezing cells by impeding the cooling

rate and decreasing generation of ice crystal inside of the cell. However, DMSO is a toxic compound and should be removed from the cell culture [50]. The pellet was resuspended in 5 ml pre-warmed growth medium and placed in a 25 cm^2 tissue culture flask (T25). The flask was incubated at 37 °C in a humidified 5% CO_2 incubator for 24 h. It is important to know the cap of tissue culture flask should be loosened slightly in the incubator for gas exchange. At 24 h, to discard the rest of DMSO, THP-1 cells were centrifuged; the pellet was resuspended in 5 ml pre-warmed growth medium, and cells were incubated.

2.2.3 Establishing growth curves of THP-1 monocytes

THP-1 cells were subcultured to initial cell densities of 1.0×10^5, 2.0×10^5, and 3.0×10^5 cells/ml, and seeded in three different 25 cm^2 tissue culture flasks. The number of cells was counted using a counting chamber every 24^{th} h for 8 days, and plotted against time.

2.2.4 Growth and experimental conditions

Human THP-1 monocytes were cultivated in maintenance tissue culture flasks with an initial density of 3×10^5 cells/ml. The cells were subcultured before they reach to 8×10^5 cells/ml (plateau phase). The cell density was not allowed to exceed 8×10^5 cells/ml in order to ensure the exponential growth. If cells exceed 8×10^5 cells/ml, the mitosis rate will

decrease, and cells may clump or have an irregular and blebbing appearance. If cells start to look like this, they should be terminated, since they will not recover [60]. Thus, the new vials of cells, from the liquid N_2 tank, would be thawed.

Based on the growth rate, cells were subcultured once or twice a week to ensure a continuous and logarithmic growth. The experience with THP-1 cells has shown that they grow very slowly after thawing and cultivation for around three to four weeks, and then grow as normal. It is maybe better to thaw two or three CryoTubes of cells simultaneously and culture in one flask in order to speed the growth process.

For maintenance or subculturing of culture, pre-warmed fresh medium was added, or medium was replaced to dilute back to 3×10^5 cells/ml [61]; it should be noted that replacing of medium is not usually performed in suspension cultures [50]. In other words, the suspension cultures are: (1) diluted and expanded, (2) diluted and the excess discarded, or (3) the high volume of the cell suspension is withdrawn and residue is diluted back to a proper seeding density [50]. These actions are applied based on how many cells are needed for performing experiments. In theory, THP-1 cells should be utilized during five passages as their characteristics might alter over time [60]. In routine, this was not observed; the morphology and properties of THP-1 cells more commonly changed when they reached an approximate passage-number of 30. Thus, in our routine, THP-1 cells were terminated before getting to a passage-number of 30, and a new batch of cells was thawed.

Prior to all experiments in this master's project, THP-1 cells were subcultured to 3×10^5 cells/ml. Then, during the next four days the cells

reached a density of ~7×10^5 cells/ml. The withdrawn cells with a density of ~7×10^5 cells/ml were centrifuged at 1600 rpm at 25 ℃ for 5 min and resuspended in pre-warmed 0.5% FBS-supplemented medium**,** as the serum starved state, prior to the different treatments.

2.3 Cell proliferation and viability methods

2.3.1 Estimating proliferation by cell counting

In this method, cell viability is validated by Trypan Blue staining [62-64]. For viability assessment, the cell suspension is diluted 1:2 in Trypan Blue dye ready-to-use solution. 10 µl cell suspension is aspirated by micropipette and diluted by pipetting with 10 µl of Trypan Blue. 10 µl of the diluted cell suspension is transferred into chamber for analysis [63].

The Bürker chamber has 9 large squares (1 mm^2 each), divided by double lines (0.05 mm apart) into 16 group squares (Figure 5). In this cell counting method, first, a cover slip was placed on the chamber and tightened carefully. The cell sample was mixed thoroughly, and 10 µl cell suspension was aspirated. The cell suspension was transferred immediately to the edge of chamber and dispensed; they were let to be drawn under the cover slip through capillary force. The chamber was not allowed to be over filled or under filled by cells, since its dimensions may change due to alteration to the surface tension. The cells were counted in minimum 4 large squares identified by the triple lines. If cell numbers in each square are close to each other, one can be calculated as the average. If numbers are not close to each other, 6 or 9 large squares would be counted. At the end of procedure, the average of counted large squares was calculated, and cell concentration per 1 ml was determined as follows [63]:

- Mean value number of cells = Y (1 square corresponds 0.1 mm^3 (1 cm^3 = 1 ml))
- Number of cells/ml = $Y \times 10^4$ [63].

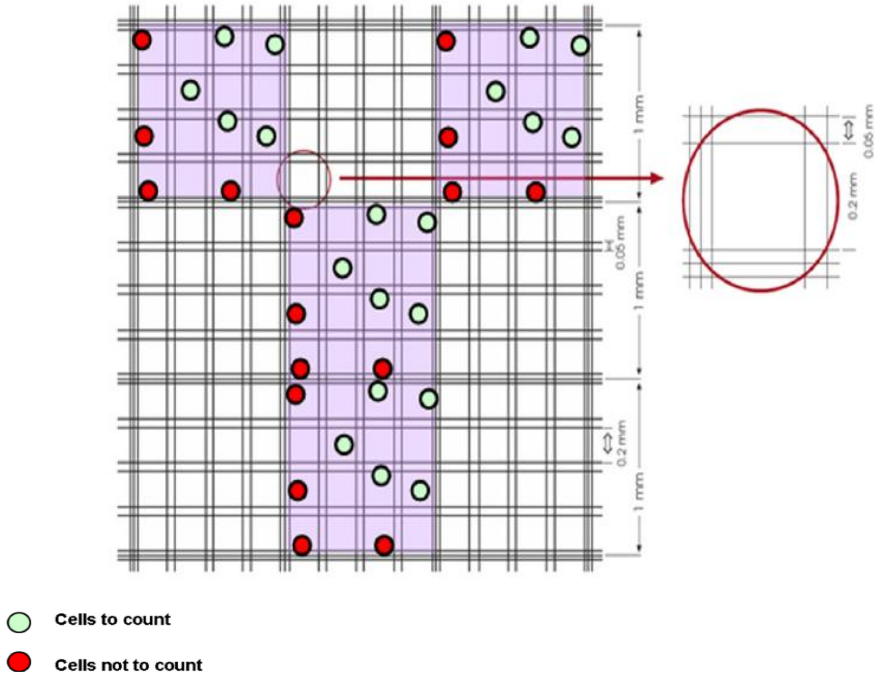

Figure 5 The surface of Bürker chamber. The Bürker chamber contains 9 large squares (1 mm^2 each), split in double lines (0.05 mm apart) into 16 group squares. The cells are counted in minimum 3 or 4 large squares, identified by the triple line and shaded in the figure [63].

Actively proliferating THP-1 cells (passage number < 30), with a density of ~7×10^5 cells/ml, were centrifuged and serum starved in 0.5% FBS-supplemented medium for 24 h. At 24 h of starvation, cells were treated

with 20 nM, 100 nM, and 1µM insulin for 24 h to 72 h. The THP-1 viable cells were counted at each exposure periods through a counting chamber.

2.3.2 Resazurin (Alamar Blue) assay to estimate cell proliferation

Resazurin (Alamar Blue) is a non-toxic, redox indicator that can be reduced, by enzymatic or chemical reaction in viable cultured cells, to make resorufin; metabolically active living cells convert a blue non-fluorescent dye (resazurin) into a pink fluorescent end product (resorufin), which accumulates in the medium [65]. Nonviable cells are not metabolically active, and do not convert the resazurin to resorufin. The specific cellular mechanisms of resazurin reduction in viable cell are unknown, but probably involve responses generating reducing equivalents such as NADH. The resazurin transforms non-fluorescent resazurin to fluorescent resorufin by mitochondrial reductase [66]. The resazurin bioassay is a non-toxic quantitative method for measuring metabolic activity, cell proliferation, viability, and cytotoxicity of cell cultures. Cells exposed to resazurin can be reverted to culture or utilized for other experiments [67-69].

Resazurin should be added equal to 10% of cell culture volume, and the change in color can be recorded at various time courses in order to determine the optimal resazurin metabolisation time in a specific cell model system. The optimal resazurin metabolization time depends on cell type (duration of cell cycle of a cell type) and its metabolic capacity [67,

70]. Longer incubation time periods may give rise to enhanced detection sensitivity, however there may be a loss in detection due to converting resorufin to hydroresorufin [67]. After an appropriate incubation time, the change in color is determined by a microplate-reading spectrophotometer, equipped with a filter set for 560-nm excitation and 590-nm emission wavelengths (in theory) [67], which is a preferred method due to providing the optimal sensitivity [67]. For data analysis, color intensity fold changes, compared to control, are plotted against stimulation time courses [67, 69, 71].

To optimize the Resazurin assay, THP-1 monocytic cells (passage number < 30), with a density of $\sim 7 \times 10^5$ cells/ml, were deprived of serum in 0.5% FBS-supplemented medium (for 0 h). 5000, 10000, and 20000 starved cells/well were seeded in a 96-well tray and treated with 1 µM INS. The 96-well tray incubated for 24 h. Following 24 h stimulation, 10 µl resazurin (equal to 10 % of content's volume of well) was added to each well and incubated for 1 h to 4 h. The color change of metabolic reduction of the blue resazurin to pink resorufin was determined at each resazurin metabolisation's exposure periods by Termo Labsystems Multiskan Ascent 354 at OD 550 with 595 nm correction. The experiments were repeated 3 times with 6 technical replicates each.

For the dose response experiments, THP-1 monocytic cells (passage number < 30) with a density of $\sim 7 \times 10^5$ cells/ml were synchronized in 0.5% FBS-supplemented medium (for 0 h). 20000 starved cells/well were seeded in a 96-well tray and treated with 20 nM, 100 nM or 1 µM INS. The 96-well tray incubated for 8 h. At 8 h, 10 µl resazurin (equal to 10% of content's volume of well) was added to each well, and the tray

incubated for 4 h resazurin metabolisation. At 4 h, the color change was measured by Termo Labsystems Multiskan Ascent 354 at OD 550 with 595 nm correction. After measuring, the plate was discarded. The process of adding resazurin and determination of metabolic reduction were repeated with different plates at 16, 24, 36, and 48 h time courses. The time points were selected based on results of cell counting.

2.3.3 Flow cytometry to analyze cell cycle phase distribution

Cell proliferation has until recent years been investigated by methods which quantify total cell division over a short time**,** or recognize cells which have recently divided, but could not ascertain how many generations have arisen, nor permit the restoration of viable cells for additional analysis [72].

The measurement of S-phase fraction (SPF) calculated from DNA histograms has been one of the earliest applications of flow cytometry to investigate cell proliferation. SPF is a sketchy approach that does not provide details of rate of cell proliferation. One of the methods of flow cytometry involves bromodeoxyuridine (BrdU) DNA incorporation that offers more detailed analysis of cell cycle and the rate of cell proliferation [73]. The total DNA staining is performed through propidium iodide (PI) and analyzed by flow cytometry that measures

cells in the various stages of the cell cycle. This method separates cells in G1-phase from S-phase and S-phase from G2/M-phase [64].

One of the flow cytometric approaches for cell cycle analysis is based on a single time point measurement of the cell population. This approach can rely on measurement of DNA content solely or in addition to DNA content, another characteristic of cells is measured. The measured characteristic is expected to provide the knowledge about metabolic or molecular attribute(s) of the cell that matches with a rate of cell progression by cycle or is a biomarker cell proliferative potential or quiescence. The single time point measurement shows the distribution of cells in G1 vs S vs G2/M, but it does not reveal direct knowledge on cell cycle kinetics. However, the length of G1, S, or G2/M phase can be evaluated from the cells percentage in the respective phase if length of the cell cycle, or duration of doubling of cells in the culture, is recognized [67]. Quantitation of the total DNA per cell is very effective in analyzing the progress of cells via the cell cycle (G1 -> S -> G2 -> M). Flow cytometry is a precise technique for sorting of cells based on DNA content [74].

THP-1 cells (passage number < 30) with a concentration of $\sim 7\times10^5$ cells/ml were resuspended in 0.5% FBS-supplemented medium. 800000 starved cells/well were seeded in a 6-well tray and treated with 20 nM, 100 nM, or 1 µM INS for 16 h to 36 h. These time-points selected according to results of resazurin assay. At each time course, cell suspension was transferred to 15 ml- tubes. The cells were centrifuged at 1600 rpm for 5 min, and the pellet was drop-by-drop resuspended in 2 ml ice-cold (-20 ℃) methanol to fix and permeate cells. With fixed cells, the

light and fluorescence scatter's properties are stable, and data acquisition can be postponed for days or weeks. Methanol also permeates cell membrane to propidium iodide (PI) [74]. The fixed cells were stored in −20 ℃ until analysis. For analysis, they were spun at 1600 rpm for 5 min. The pellet was resuspended in 1.5 ml of 200 µg/ml RNase and left in room temperature for 30 min in order to discard RNA. The content of tube was spun at 1600 rpm for 5 min, and supernatant was discarded. The pellet was resuspended in 1 ml of 40 µg/ml PI and left for a proper DNA staining in a dark environment for 15 min; PI is sensitive to the light. After 15 min, all samples were covered with aluminum foil and kept in refrigerator until the measurement by a flow cytometer. The analyses of DNA content and cell cycle phase distribution were performed in three independent experiments (n = 3) using the Beckman Coulter flow cytometer with 20000 cells (events) per sample analyzed. The percentage of cells in the G1-, S- and G2/M-phases quantified by the software Kaluza v1.1.

2.4 Statistical analysis

Statistical analyses of cell counting tests, resazurin assays, and flow cytometry tests were performed using t-test with 95% confidence interval in SPSS (IBM SPSS Statistics 21); the p values ≤ 0.05 were considered significant.

3 RESULTS

3.1 The growth curve of THP-1 cells

The optimal method of determining the proper seeding concentration is to carry out a growth curve at different seeding densities and thereby determine the density that will present a very short lag phase and early entry in rapid log phase (a short population-doubling time) but will reach the top of the log phase at a time that is suitable for the next subculture [50].

THP-1 cells were subcultured to initial cell densities of 1.0×10^5, 2.0×10^5 and 3.0×10^5 cells/ml. The number of cells was counted using a counting chamber every 24 hours for 8 days, and plotted against time. As shown in figure 7, cells that were seeded into 3.0×10^5 cells/ml entered the log phase immediately, while cells with initial density of 1.0×10^5 and 2.0×10^5 were in the lag phase the first 24 hours. Cells with an initial density of 3.0×10^5 also had a short log phase compared to others and reached near the top of log phase at 96 h, a convenient time-period for starting an experiment or the next subculture. Thus, seeding density of 3.0×10^5 cells/ml was selected as an ideal seeding density for a cell maintenance flask prior to experimental use or the next subculture. For cells with a seeding density of 3.0×10^5 cells/ml, a plateau phase was observed when cells entered a density of 8×10^5 cells/ml. Cells for experimental procedure should be withdrawn in near the top of log phase before they have entered the plateau phase, in order to ensure that cells

are in an actively proliferating state. As a result, cells should be taken for experiments when they reach to a density of ~7× 10^5 cells/ml (Figure 6).

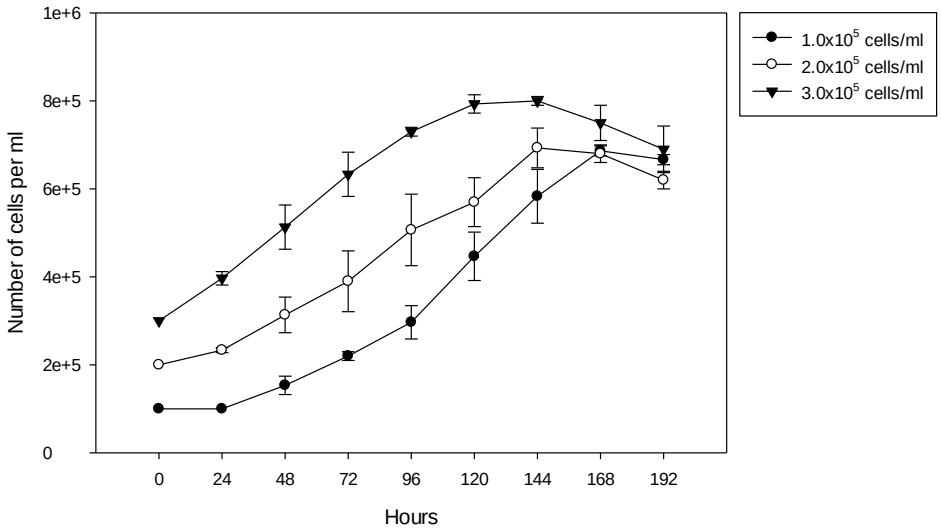

Figure 6 Growth curves obtained from three different seeding densities (1.0×10^5, 2.0×10^5 and 3.0×10^5 cells/ml) of THP-1 cells by cell counting. The cell density is represented as the mean ± SD of three independent experiments (n=3). Error bars denote ± SD.

3.2 Insulin increases proliferation in THP-1 cells

Hyperproliferation of monocytes has been implicated in CVD [75, 76]. As introduced previously, there is a link between obesity and/or T2D and insulin resistance-associated hyperinsulinemia [14]. Obesity and T2D are two risk factors for CVD [5]. In this study we aimed to clarify if there is a relationship between the high levels of insulin and hyperproliferation of monocytes.

By cell counting, we measured changes in cell proliferation in response to insulin after 24, 48 and 72 h. Following 24 h, 100 nM insulin significantly increased cell proliferation (23 % increase in cell numbers, n = 5, * p = 0.01 - 0.05). Cells significantly responded to 10 % FBS by 36 % increase in cell numbers (n = 5, ** p = 0.001 - 0.01). The treatment with 20 nM insulin did not affect cell proliferation. 1 µM insulin treatment resulted in 13 % non-significant increase in cell numbers (Figure 7 A).

Following 48 h, treatment with 20 nM and 100 nM insulin did not affect cell proliferation at all. Cells treated with 1 µM insulin did not show a significant increase in cell proliferation (11 % non-significant increase in cell numbers). The cells responded to 10 % serum by significantly increasing cell numbers by 45 % (n = 5, ** p = 0.001 - 0.01) (Figure 7 B).

At 72 h, the cells did not respond to 20 nM, 100 nM and 1 µM insulin treatment. The treatment of cells with 10 % FBS induced a significant increase in cell numbers by 71 % (n = 5, *** p < 0.001) (Figure 7 C). See Appendix A for data as means ± SD.

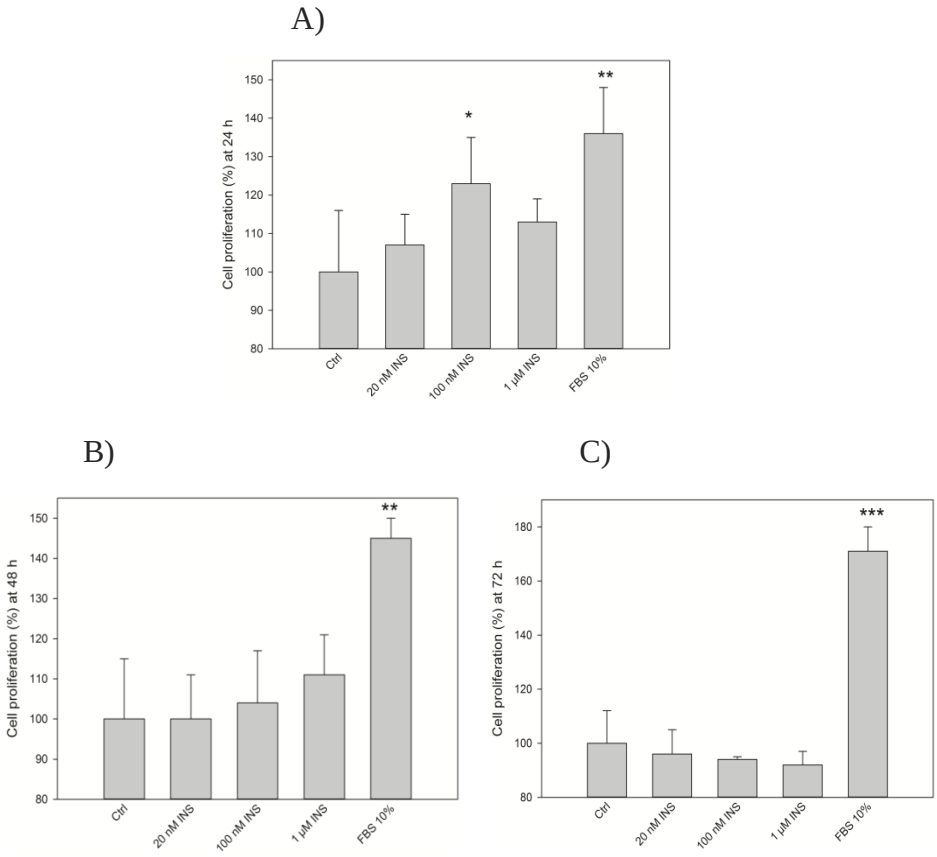

Figure 7 Dose- and time course-dependent changes in cell proliferation, as shown by cell counting. **a** Following 24 h of treatment, 100 nM insulin was found to significantly increase cell proliferation. **b** Following 48 h, a non-significant trend was found towards an increase in insulin-stimulated proliferation in response to 100 nM and 1 µM INS, but not at 20 nM INS (no effect at 20 nM INS). **c** Following 72 h, there was a non-significant trend towards a decrease in insulin-induced proliferation in response to 20 nM, 100 nM and 1 µM INS treatments. The data is represented as mean ± SD where Ctrl is set to 100 % proliferation (n = 5). * p = 0.01 - 0.05, ** p = 0.001 - 0.01, *** p < 0.001 versus untreated cells. INS, insulin; Ctrl, untreated cells.

In summary, insulin-induced proliferation was the most potent at 24 h at 100 nM insulin. This stimulatory effect on proliferation was reduced following longer exposure periods. Based on results of cell counting, there was an increased trend of insulin-induced proliferation at each time-point of 24 h and 48 h (except from 20 nM insulin treatment at 48 h), an effect was no longer evident following 72 h of treatment; rather, there was a non-significant trend in which insulin reduced proliferation following 72 h.

3.3 Insulin treatment may not change THP-1 cell morphology

We also inspected cells while counting cells in order to find whether insulin affects morphology of THP-1 monocytes. We monitored each culture flask related to each insulin treatment (20 nM, 100 nM and 1 µM INS) and compared to untreated cells by a microscope following 24, 48 and 72 h. We found that insulin did not change THP-1 cell morphology and color of culture medium. Insulin treatment did not stimulate cell adhesion to the bottom of culture flasks or clustering of cells (Figure 8).

Ctrl

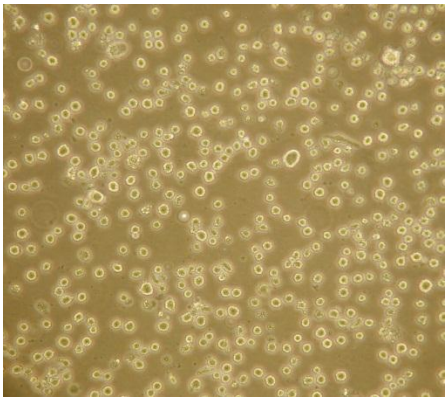

FBS 10%

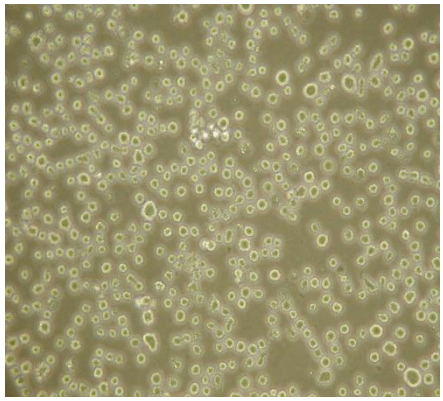

20 nM INS

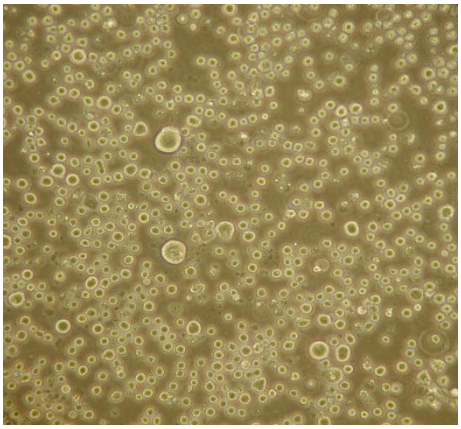

100 nM INS

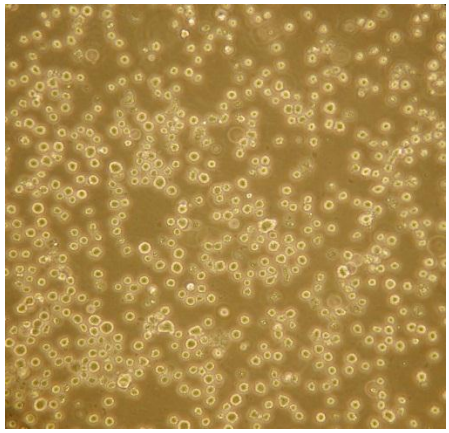

1 μM INS

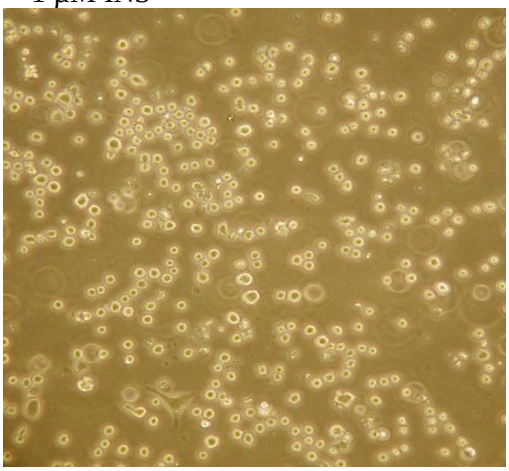

Figure 8 There were no significant differences between cell morphology of each of insulin treatment (20 nM, 100 nM and 1μM INS) and cell morphology of untreated cells following 24 h. The photos were taken from one representative experiment. (×20).

3.4 Optimization of time of resazurin metabolization and cell-seeding density

Having shown by cell counting that insulin may increase proliferation in THP-1 cells, we aimed to confirm the finding by the use of resazurin as an indicator of metabolic activity or proliferation. Thus, the results of resazurin assays must be confirmed by an additional method, in order to demonstrate whether possible resazurin metabolization is due to increased metabolic activity or proliferation. First we performed a series of resazurin assays to identify the experimental conditions (time of resazurin metabolization and cell-seeding density) where insulin-induced metabolic activity is most evident. It is important to consider that an

increased metabolic activity may indicate cell proliferation or a state of metabolically-active living cells [67, 68].

In these series of experiments, all insulin-treatments were performed at 1 µM insulin. Following 24 h of insulin treatment of cells and 1 h of resazurin metabolization, we found that insulin significantly increased the metabolic activity in cells seeded at 20000 cells/well by 5 % ($n = 3$, *** $p < 0.001$), whereas insulin did not affect metabolic activity in cells seeded at 5000 and 10000 cells/well (Figure 9 A).

It seems 10 % FBS-supplemented medium (FBS 10 %) significantly decreased resazurin metabolization in all varying seeding densities (5000, 10000 and 20000 cells/well) and in all time courses (24 h insulin treatment and 1- 4 h resazurin metabolization) relative to untreated cells. That may be explained by extensive cell metabolic activity leading to formation of hydroresorufin which is colorless and not detected spectrophotometrically [67] (Figure 9 A-D). To minimize this phenomenon, the proportion of FBS was reduced to 2 %, and the effect of 2 % FBS was investigated in the next section (3.5).

After 24 h of insulin treatment of cells and 2 h of resazurin metabolization, the cells at 20000 cells/well responded to the insulin treatment by significantly increasing their metabolic activity by 5 % ($n = 3$, *** $p < 0.001$) while cells seeded at 10000 and 5000 cells/well did not respond to insulin (Figure 9 B).

Following 24 h of insulin treatment of cells and 3 h of resazurin metabolization, insulin significantly increased metabolic activity in

20000 cells/well by 8 % (n = 3, *** $p < 0.001$), whereas insulin did not affect metabolic activity at 10000 and 5000 cells/well (Figure 9 C).

After 24 h of insulin treatment and 4 h of resazurin metabolization, insulin induced a significant increased metabolic activity in 20000 cells/well by 9 % (n = 3, *** $p < 0.001$) while the cells seeded in 10000 and 5000 cells/well did not respond to insulin (Figure 9 D). See Appendix B for data as means $\pm$ SD.

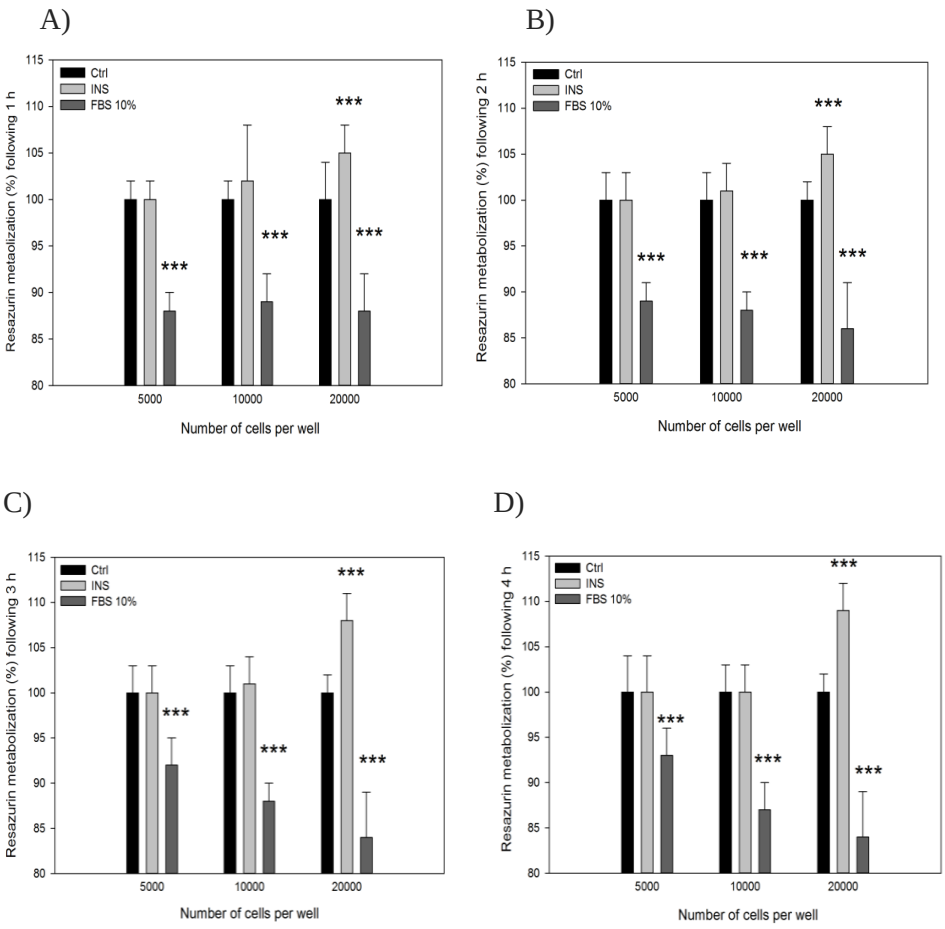

Figure 9 Insulin treatment (1 µM) significantly increased the metabolic activity in the cells seeded in 20000 cells/well that is most evident following 24 h of insulin treatment and 4 h of resazurin metabolization (**d**), as shown by resazurin assay. Insulin (1 µM) did not affect metabolic activity in the cells seeded in 5000 and 10000 cells/well following 24 h of insulin treatment and 1-4 h of resazurin metabolization. The resazurin metabolization is indicated as mean ± SD where Ctrl is set to 100 % metabolic activity (n = 3). *** $p < 0.001$ versus untreated cells. INS, insulin; Ctrl, untreated cells. **a, b, c & d** The cell metabolic activity following 24 h of insulin treatment and 1, 2, 3 and 4 h of resazurin metabolization, respectively.

We observed a trend that metabolic activity increases when the seeding density increases. The insulin-induced metabolic activity was found to be most apparent in 20000 cells per well at 4 h of resazurin metabolization. We selected these experimental conditions as the ideal seeding density and ideal time of resazurin metabolization for performing subsequent resazurin assays in order to investigate the most potent dose of insulin treatment.

3.5 Insulin increases metabolic activity in THP-1 cells

Having shown by cell counting that insulin increases cell proliferation, it was required to confirm or support that finding. Based on results of previous resazurin assays in section 4.4, we performed a series of resazurin assays to investigate if insulin induces metabolic activity in a dose- and time-dependent manner, as the increased metabolic activity may represent the proliferation of cells or a general activation of viable cells [67, 68, 77]. THP-1 cells (20000 cells/well) were serum starved prior to treatment with varying doses of insulin (20 nM, 100 nM and 1 µM) in 96-well trays for 8 h to 36 h before 4 h resazurin metabolization in order to investigate the most potent dose of insulin. We selected 2 % FBS as the positive control of experiments, since resazurin metabolization was not detected by 10 % FBS in previous resazurin assays.

At 8 and 16 h, the varying doses of insulin (20 nM, 100 nM and 1 µM) did not affect cell metabolic activity (Figure 10). We found a (non-significant) trend of increased metabolic activity at 2 % FBS for 8 and 16 h time-points (data not shown).

At 24 h, 20 nM and 100 nM insulin treatments induced significant increases in the metabolic activity by 5 % for each treatment (n = 4, ** p = 0.001 - 0.01). The cells did not respond to 1 µM insulin treatment. There was no significant difference between 20 nM and 100 nM insulin-induced cell metabolic activity. We found that 20 nM and 100 nM insulin-treated cells significantly were different from 1 µM insulin-treated cells in their metabolic activity (Figure 10). 2 % FBS significantly increased the cell metabolic activity by 9 % relative to untreated cells (data not shown). Hence, the interpretation regarding effect of 10 % FBS, in previous section, was confirmed. The metabolic activities were attenuated following longer exposure period (after 36 h) of insulin and serum treatments (data not shown). See Appendix C for data as means ± SD.

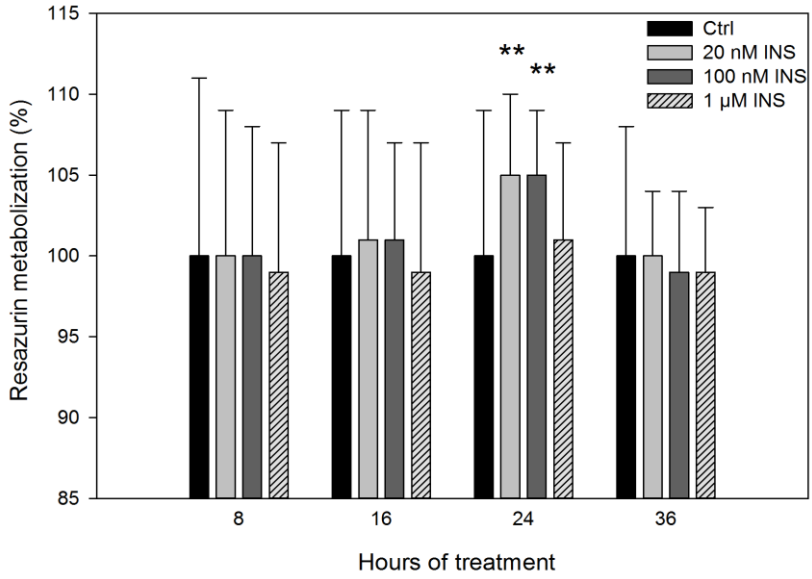

Figure 10 Insulin-induced metabolic activity appears to be the most potent at 24 h at 20 nM and 100 nM insulin. These stimulatory effects, on the metabolic activity of cells, were reduced following longer incubation period, as shown by resazurin assay. The resazurin metabolization is indicated as mean ± SD where Ctrl is set to 100 % metabolic activity. For 8 h (n = 3), for 16 and 36 h (n = 4), for 24 h (for Ctrl and 1 µM INS, n = 7. For FBS 2%, 20 nM INS and 100 nM INS, n = 4). ** p = 0.001 - 0.01 versus untreated cells and 1 µM INS-treated cells. INS, insulin; Ctrl, untreated cells.

3.6 Insulin treatment alters cell cycle phase distribution in THP-1 cells in support of onset of mitosis

Increased metabolic activity shown by resazurin assay in section 4.5 may indicate cell proliferation or a general activation of cells. Hence, we performed flow cytometry to determine whether the increase in metabolic activity measured by resazurin assays were due to an increased cell activation or cell proliferation [67].

By flow cytometry, we analyzed the effect of insulin in cell cycle phase distribution. The cell cycle phase distribution following 16 h of 100 nM insulin treatment is shown as a representative analysis of cell cycle phases (Figure 11, A-D).

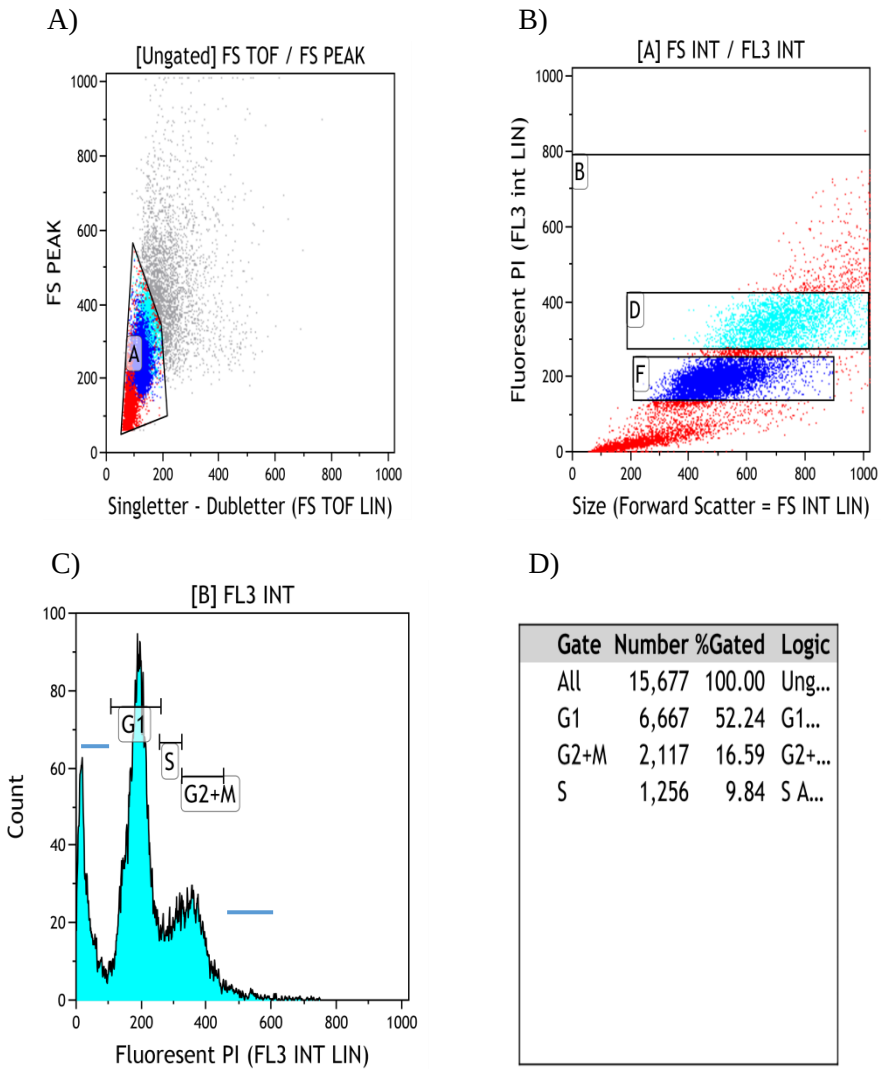

Figure 11 Dot plots and histograms of cell cycle phase distribution obtained from the Beckman Coulter flow cytometer and Kaluza v1.1 software. The dot plots and histograms refer to one sample from one experiment following 16 h of 100 nM INS treatment. In this figure, the general process was that PI-stained cells were subjected to gated major population from the histograms A and B, and they showed gated cells on histogram C. A) The cellular debris and/or doublet cells are in part circumvented by the correct forward/side scatter signals. Doublets were detected by collecting forward scatter peak (Y-axis) against integrated signals (X-axis). FS, forward scatter; TOF, time of flight; Singletter, single cells; Doubletter, doublet cells. B) Dot plot gating to exclude subcellular debris and/or clumps using fluorescent intensity of Propidium Iodide- (PI)-stained cells (Y-axis) against size of cells (X-axis) estimated by forward scatter. The combination of fluorescent and scattered light were detected and analyzed. FL3, fluorescent channel3; INT, intensity C) The gated cells on the fluorescent (FL3) histogram. Fluorescence intensity was detected in all cells at channel FL3 for PI. Count, cell numbers. D) Total gate was set manually to exclude cell debris and/or aggregates of cells from percentages of cell cycle phases. – denote cell debris and/or aggregates of cells.

For flow cytometry data analysis, total gated phases were set to exclude cell debris and/or aggregates of cells from final analysis and percentages of cell cycle phases. In addition, total gated phases were defined to 100% in each sample, and each respective phase was calculated relative to that. Thus, the percentages of G1+S+G2/M add up to 100% in each sample. All data is presented in the table 2 below.

Table 2 Effect of insulin on cell cycle phase distribution.

	G1 (%)	S (%)	G2/M (%)	S+G2/M (%)
16 h				
Ctrl	65.35 ± 2.70	18.24 ± 2.02	16.41 ± 0.92	34.65 ± 2.70
20 nM INS	59.73 ± 6.08	23.49 ± 3.86	16.78 ± 4.53	40.27 ± 6.08
100 nM INS	62.78 ± 9.35	22.41± 4.29	14.80 ± 5.96	37.22 ± 9.35
1 µM INS	65.24 ± 2.52	17.29 ± 0.48	17.47 ± 2.49	34.76 ± 2.52
FBS 2 %	62.61 ± 4.28	18.14 ± 3.78	19.24 ± 4.48	37.38 ± 4.29
FBS 10 %	65.58 ± 4.22	19.56 ± 1.70	14.86 ± 4.00	34.42 ± 4.22
24 h				
Ctrl	67.38 ± 2.38	19.39 ± 2.19	13.23 ± 3.03	32.62 ± 2.38
20 nM INS	63.51 ± 6.57	20.28 ± 3.32	16.21 ± 3.94	36.49 ± 6.57
100 nM INS	59.87 ± 1.63*	22.25 ± 1.85	17.88 ± 2.50	40.13 ± 1.62*
1 µM INS	66.41± 3.77	13.75 ± 1.67*	19.84 ± 2.91	33.59 ± 3.77
FBS 2 %	68.04 ± 2.14	14.59 ± 3.20	17.37 ± 4.80	31.96 ± 2.14
FBS 10 %	64.55 ± 4.76	13.71 ± 2.22*	21.73 ± 3.98*	35.45 ± 4.76
36 h				
Ctrl	54.33 ± 9.84	24.01 ± 5.17	21.67 ± 4.91	45.67 ± 9.84
20 nM INS	48.15 ± 3.28	26.39 ± 2.08	25.46 ± 3.11	51.85 ± 3.28
100 nM INS	48.46 ± 2.46	23.90 ± 3.64	27.65 ± 2.00	51.54 ± 2.46
1 µM INS	49.52 ± 2.48	31.24 ± 1.82	19.25 ± 0.66	50.48 ± 2.48
FBS 2 %	58.29 ± 10.06	22.27 ± 5.61	19.44 ± 5.62	41.71 ± 10.06
FBS 10 %	63.75 ± 5.92	17.79 ± 3.55	18.46 ± 5.02	36.25 ± 5.92

The data present the percentages of mean ± SD (%) of three independent experiments (n=3). The asterisks denote a significant difference from the respective untreated cells (* p = 0.01- 0.05). INS, insulin; h, hours.

Following 16 h, each treatment (FBS 2%, FBS 10%, 20 nM, 100 nM and 1 μM INS) did not significantly alter the amount of cells in G1, S and G2/M compared to untreated cells. There were no significant differences between the mitotic index (S+G2/M) in response to each treatment (FBS 2%, FBS 10%, 20 nM, 100 nM and 1 μM INS) and the mitotic index (S+G2/M) in untreated cells (Table 2) (Figure 12 A).

In contrast, following 24 h and compared to untreated cells, 100 nM INS treatment significantly shifted cell phase distribution towards fewer cells in G1-phase (n = 3, * p = 0.01- 0.05), whereas we observed a non-significant trend towards more cells in S- and G2/M-phases. However, the proportion of cells in S+G2/M in response to 100 nM INS significantly was more than the proportion of cells in S+G2/M in untreated cells (n = 3, * p = 0.01- 0.05). Taken together, this finding is in agreement with the results from the cell counting and resazurin assay, confirming that insulin (at 100 nM at 24 h) significantly increased a mitotic effect in THP-1 monocytic cells. Compared to untreated cells, 1 μM INS treatment significantly shifted cell phase distribution towards fewer cells in S-phase (n = 3, * p = 0.01- 0.05), whereas INS did not significantly alter the amount of cells in G1- and G2/M-phases or S+G2/M. In response to FBS 10 %, significantly fewer cells were found in S-phase (n = 3, * p = 0.01- 0.05), whereas significantly more cells were accumulated in G2/M-phase (n = 3, * p = 0.01- 0.05). Hence, this finding may support the onset of cell growth and proliferation in response to serum 10 %, although serum 10% did not significantly reduce amount of cells in G1-phase. Each treatment of FBS 2% and 20 nM INS did not significantly alter cell cycle phase distribution compared to untreated cells (Table 2) (Figure 12 B).

Finally, after 36 h, each treatment (FBS 2%, FBS 10%, 20 nM, 100 nM and 1 μM INS) did not significantly alter the amount of cells in G1, S and G2/M compared to untreated cells. There were no significant differences between S+G2/M in response to each various treatment (FBS 2%, FBS 10%, 20 nM, 100 nM and 1 μM INS) and S+G2/M in untreated cells (Table 2) (Figure 12 C).

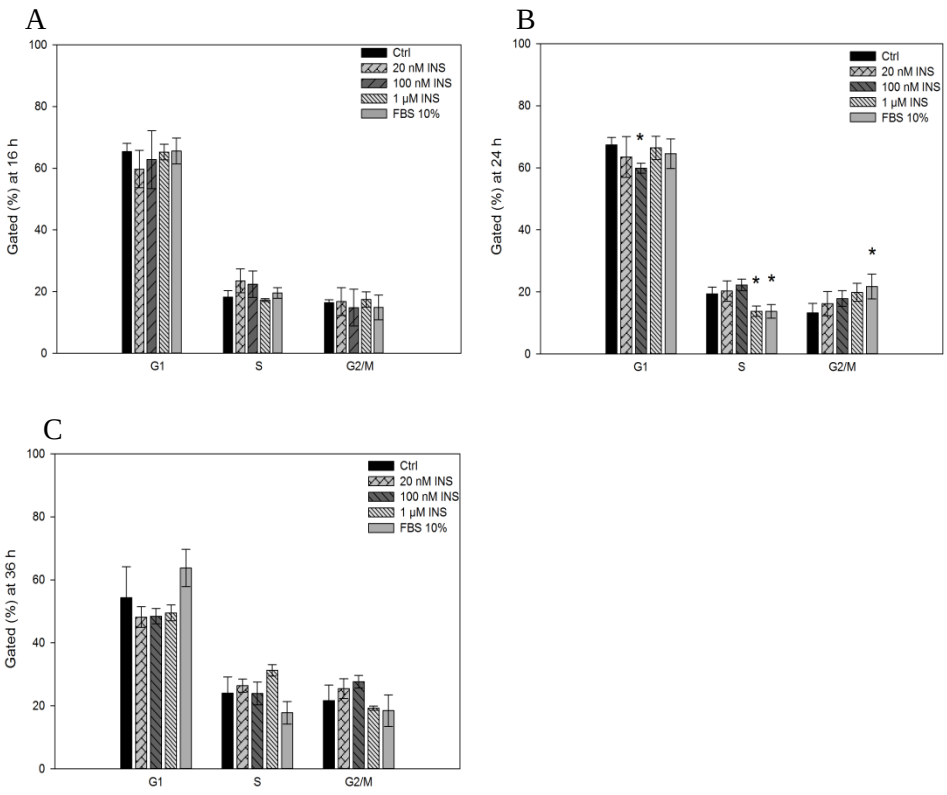

Figure 12 The concentration- and time-dependent alterations in the THP-1 cell cycle phase distribution, as shown by flow cytometry. The data represent percentages of mean ± SD (%) of three independent experiments (n = 3). * p = 0.01 - 0.05 versus untreated cells. **a** Following 16 h, none of treatments significantly altered cell cycle phase distribution compared to untreated cells. **b** After 24 h, each of treatments of 100 nM, 1µM INS and FBS 10% significantly altered cell cycle phase distribution. **c** Following 36 h, none of treatments significantly changed cell cycle phase distribution.

4 Discussion

4.1 THP-1 monocytes represent a suitable model-system for investigating the effect of insulin on monocytes

THP-1 cells technically have some advantages over human primary monocytes. These benefits have been taken into account before this study was conducted: First, the homogenetic background of THP-1 cells minimizes the rate of variability in the cell phenotype. This characteristic is crucial when studying function of biochemicals with high variability [78], such as insulin. A cell line with relative minimal variability in the cell phenotype gives the most reliable findings. Second, THP-1 cells can be stored in liquid nitrogen for several years. Following a proper procedure, this cell line would be restored without apparent effect on monocyte characteristics and cell viability. The ability to store cells ensures enough cells for DNA, RNA, and protein studies [78]. Third, this cell line has been already established as a proper cell model for metabolic studies by our research group. In contrast, there is a limitation in the availability of primary human monocytes; accounting for only 3-9% of all leukocytes. Additional challenges for the employment of primary cells include: a) the donor accessibility and variability; b) the difficulty to acquire large amounts of pure monocytes in humans [43]; c) the contamination with other blood constituents (such as platelets); d) a restricted-survival period in the culture [78].

Other immortalized human monocytic cell lines also exist, including ML-2, U937, and Mono Mac 6 cells. However, THP-1 cells demonstrate a

more mature monocytic phenotype [78] and serve as a supplementary model-system and relevant surrogate tissue for circulating blood leukocytes for *in vitro* mechanistic studies [3]. These findings suggest that undifferentiated THP-1 monocyte cultures are as a suitable model-system to investigate the effect of high levels of insulin, at the cellular level. The monocytes may prove to be appropriate tools for studying insulin defects that lead to insulin resistance, obesity-associated type 2 diabetes, CVD, and cancer. This is important because the escalated incidence of obesity, insulin resistance, T2D and other metabolic diseases in the western world calls for a better understanding of the mechanisms underlying these disorders and the outcomes thereof [54-56]. The increased incidence of metabolic diseases place a pressure on the scientific community for prevention and early therapeutic intervention [79].

4.2 Monocytes respond to insulin

Insulin is well known as an anabolic hormone that reduces the level of blood glucose. It is also a potent growth factor and anti-apoptotic factor that regulates gene expression in various cells [80]. The cellular effects of insulin in THP-1 monocytes were investigated in this study. THP-1 cells respond to high levels of insulin by significantly increasing cell numbers and proliferation, in otherwise serum starvation leads to a reduced cell numbers, as shown by cell counting. Resazurin assays support that insulin stimulates proliferation in THP-1 monocytes as the insulin-treated cells significantly increased metabolic activity by 5 %. Flow cytometric

cell cycle analysis also confirms that insulin induces activation of cells in favor of the mitosis onset, as insulin significantly altered the portion of cells in the S and S+G2/M phases compared to untreated cells. However, there are tiny differences in a fraction of cells in S and G2/M phases between insulin-treated cells and untreated cells. All responses of THP-1 cells to insulin occur in a dose- and time course-dependent manner. For metabolic activity, cells respond to insulin in a seeding density-dependent fashion as well. The significant differences in metabolic activity and cell cycle phase distribution [77] between insulin-treated cells and untreated cells are still small percentages. The findings of this study regarding the increased metabolic activity in response to insulin are consistent with findings of Anide Johansen, a former master student at the lab. She studied the cellular effects of insulin in SW982 fibroblast-like synoviocytes and reported insulin increases metabolic activity of SW982 cells in a time-, dose- and seeding density-dependent manner [81].

PI3-kinase/Akt signaling pathway has been demonstrated to play a crucial role in cell survival and proliferation effects of insulin (high insulin levels) and other growth factors (such as IGF-1) in some cell types [80-83], including anti-apoptotic effect of insulin in THP-1 macrophages [80, 84]. On the other hand, a selective post-receptor defect involving the impaired PI3-kinase signaling with an unaltered MAP-kinase pathway has been shown in the macrophages and vasculature of insulin resistance/diabetic animal models as well as in skeletal muscle biopsies from insulin-resistant patients. The impaired PI3-kinase but intact MAP-kinase signaling also has been reported to facilitate insulin-mediated VSMCs and ECs migration *in vitro* [85]. The activation of

MAP-kinase pathway has been involved in proliferation, migration and inflammation of VSMCs derived from human coronary arteries in response to insulin [23]. Gogg et al. [58] recently documented a "selective" insulin resistance involving PI3-kinase signaling concomitant with increased MAP-kinase activity in type 2 diabetes microvascular ECs [23]. In addition, it has been demonstrated that insulin does not affect viability and proliferation of human coronary artery endothelial cells (HCAECs), human coronary smooth muscle cells (HCSMCs) [86], and ECs of saphenous vein [4], whereas some studies have documented increased proliferation of VSMCs of the arterial wall [23] and SMCs of saphenous vein [4] in response to insulin. The findings of all aforementioned studies might therefore be reconciled by taking into account species differences, cell and receptor (IR and/or IGF-1R) types, how they integrate and process the signal, relevancy of cell types, insulin levels [3, 4, 49, 87], and *in vitro* and physiological *in vivo* conditions [3].

Diet high in easily absorbed carbohydrates primarily increases secretion of insulin [3, 52]. Hyperinsulinemia is suggested as an important risk factor for atherosclerosis [4, 80] and CVD in diabetic patients through inhibited apoptosis in THP-1 monocytes [85] and increased SMC proliferation [88]. Hyperproliferation due to high levels of insulin on monocytes, as a finding of the current study, may be valuable information for nutritionists, physicians and CVD patients to reduce the incidence and progression of CVD.

Recent human cancer genomic analyses have revealed that many components of PI3K signaling pathway are frequently mutated in

common human tumors [89]. This alteration stimulates high rate of cell survival and proliferation, which indicate both cancer [90]and atherosclerotic lesion formation and CVD. This finding also may propose a possible role of insulin signaling in both cancer and CVD. PI3K/Akt signaling has been reported to be over-activated in some human cancers that are associated with obesity, insulin resistance and hyperinsulinemia [89-94]. These findings may indicate a crucial role for insulin in cancer and CVD. Figure 14 demonstrates a mechanistic overview of the relation between obesity, energy balance and cancer [94]. The cell counting, resazurin assays, and flow cytometry results of the present study may be an outcome of hyperinsulinemia signaling through activation of PI3K/Akt, triggering increased cell growth and proliferation. The increased proliferation may lead to CVD and cancer.

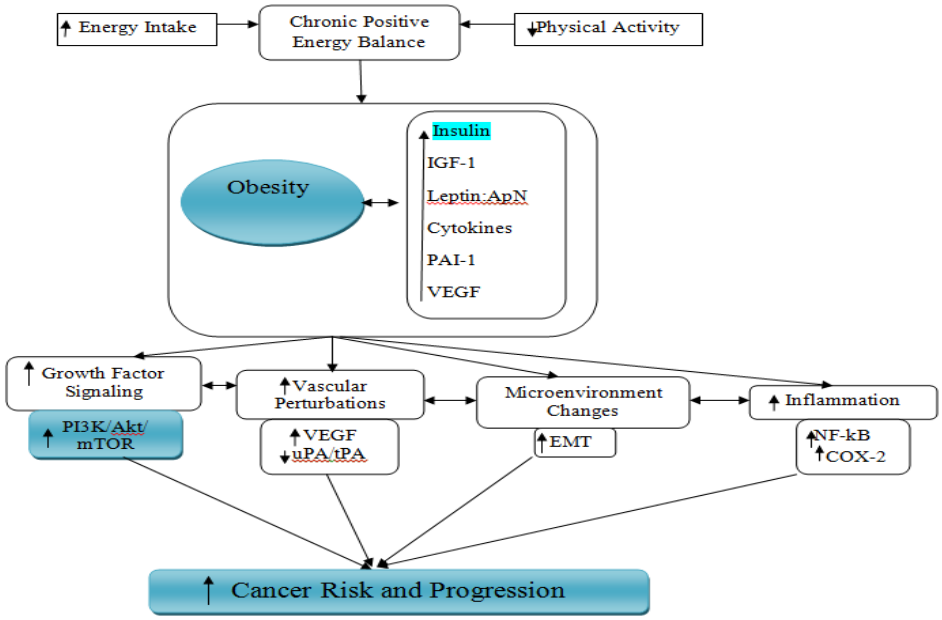

Figure 14 Obesity, energy balance, and cancer: a mechanistic overview. An arrow preceding text indicates a directional effect (e.g., activity or concentration). IGF-1, insulin-like growth factor-1; ApN, adiponectin; PAI-1, plasminogen activator inhibitor-1; tPA, tissue-type plasminogen activator; uPA, urokinase-type plasminogen activator; VEGF, vascular endothelial growth factor; PI3K, phosphoinositide 3-kinase; COX-2, cyclooxygenase-2. The relevant information to this master's project was highlighted. Modified figure [94].

4.3 Insulin treatment and THP-1 monocytic morphology

Preincubation of endothelial cell line EAhy 926 with IGF-1 suppresses human monocyte adherence in a time course- and concentration-dependent manner. Insulin at concentrations up to 10 µM does not have any significant effects on monocyte adhesion [95]. The microscopic observations of the present study are consistent with findings of

aforementioned literature, and demonstrated that each insulin treatment (20 nM, 100 nM and 1 µM) does not promote adhesion of monocytes to bottom of tissue-culture flasks, and does not alter morphology of monocytes. These observations suggest insulin may not trigger differentiation of monocytes into macrophages, hence support a role for insulin in monocyte proliferation. However, specific methods such as adhesion assay, migration assay, and confocal microscopy must be carried out to validate our observation and possible implication.

4.4 Choice of insulin concentrations

The concentrations of insulin after a meal in normal and insulin-resistant individuals are ~0.3- 0.4 nM and ~1.4- 1.5 nM, respectively [4]. Several studies have reported using various insulin concentrations from 10^{-1} nM to 10^{6} nM in different *in vitro* cell cultures [3, 80, 86, 96]. Insulin doses of 20 nM, 100 nM, and 1µM were used in the present study in order to mimic a hyperinsulinemic condition. The reason for choosing these high concentrations of insulin, which are still more than hyperinsulinemia level in human, is that high concentrations of insulin are often required *in vitro* to detect functional cellular effect; this probably reflect the differences between *in vitro* functional experiments and *in vivo* condition [4]. We found 100 nM insulin leads to the largest increase in THP-1 monocyte proliferation and does not have any cytotoxic effect. 100 nM insulin also presents the most reproducible result. Insulin affects cell proliferation in a dose- and time-dependent manner.

4.5 Selection of cell-seeding densities for growth curves and cell counting

The experience of former students at lab was utilized to determine proper cell densities that should be seeded at tissue flasks at 0 h. Three different densities were selected to cover saturation from low to high. The cells with initial seeding density of 1.0×10^5 cells/ml reached log phase and the top of log phase following 24 h and 144 h, respectively, as this initial cell density was expected to have difficulty to proliferate. The cells with initial seeding density of 3.0×10^5 cells/ml reached log phase and top of log phase immediately and following 96 h, respectively (Figure 7). These results may suggest that initiation of THP-1 monocyte proliferation depends on indirect cell to cell and cell to extracellular matrix (ECM) interactions. There are different types of cell-cell adhesion proteins that facilitate intercellular interactions, including cadherins, selectins, integrins and immunoglobulin receptors [49]. Integrins also regulate cell to ECM communication [97]. The cells with initial seeding density of 1.0×10^5 cells/ml struggled to proliferate that may be outcome of struggling with establishing intercellular and cell-ECM communications, whereas the cells with initial seeding density of 3.0×10^5 cells/ml immediately set these communications and speeded up proliferation rate. It can be reported that there is a direct correlation between initial seeding density and rate of proliferation. The similar correlation was observed in subsequent resazurin optimization assays with regard to metabolic activity (Figure 10). Finally, the initial seeding density of 3.0×10^5 cells/ml was selected to perform subsequent cell counting experiments as

this density may present more natural manner of monocytes in human vasculatures (Figure 8).

After some subculturing (passages) of cells in the same tissue culture flask, we observed that cells reach log phase and top of log phase earlier than some initial cell subcultures (passages). Initiation of cell proliferation may depend on cell-cell and cell-ECM communications that take some time to be provided. Thus, a used flask probably has already established the cell-ECM interaction that reduces the time to reach log phase and top of log phase as well [81]. This also can propose that proliferation of THP-1 monocytes firmly rely on the cell-ECM interaction.

4.6 Choice of the resazurin assay and the technical pitfalls

Resazurin and MTT assays are two viability bioassays that can be used to assess metabolic activity of cells. Resazurin assay has some advantages in comparison with MTT: non-toxic, labor-saving, safe for the user, high sensitivity, and linearity [98]. However, the detected product in MTT assay is more stable than resazurin assay. MTT is not soluble in culture medium and is best suited for adherent cell lines. Assay chemistry could determine which assay may be more suited to particular cell line or may be more applicable to adherent cells than suspension cells. In summary, suitability must be taken to account for each application and cell model [70]. The Alamar Blue (resazurin) has been utilized for measuring

immune cell proliferation and function such as monocytic cell lines. This assay does not require cell lysis and continuous assessment through time-dependent experiments is possible [70]. Based on the aforementioned information, resazurin bioassay was selected for performing the experiments of present study.

The accuracy of the resazurin assay depends on some matters: precision of cell seeding, tapping well-tray immediately after adding resazurin to make a homogenous content, and an equal atmosphere throughout well-tray. Thus, we applied a digital multi-channel pipette to ensure seeding same cell density to each well, and the aspiration/dispense of cells was always inspected. The seeding of outer edge-wells of tray was avoided and filled with PBS instead in order to guarantee an identical environment all over of well tray. The trays were returned to the incubator with considering same atmosphere surrounding each tray so the temperature and humidity were alike for each of trays. In addition, microscopic observations confirmed resazurin results.

4.7 Technical pitfalls of in vitro cell culture-based experiments

It should be noted there is a risk of inconsistent results when performing *in vitro* compared to *in vivo* experiments. *In vitro* studies are not fully representable for what occurs in the human body. The system in multicellular animals is also responsive to extracellular signals from other cells and/or cell types inducing cell division when more cells are required, and suppressing cell division when they are not required [49].

The handling of cells, mechanical stress, the state of health of cells, pH-changes, the differences in quality of batch of cells stored in liquid nitrogen, and other factors are hard to control and may affect results of *in vitro* cell culture-based experiments providing inconsistent and/or false results. It should be taken into consideration that there are some inherent limitation to *in vitro* studies, and the clinical relevance of the *in vitro* findings needs further investigation. Clinical studies could be sought to substantiate the hypothesis [23].

5. Conclusion

In conclusion, the present study shows that monocytes are responsive to insulin. Insulin appears to increase cell numbers and the metabolic activity of monocytes that may be correlated with mitotic responses and monocyte proliferation. These responses to insulin occur in a time- and dose-dependent manner, within the range of high insulin levels. Hyperproliferation of monocytes due to high levels of insulin may affect important aspects of monocyte function, for instance immune and vascular function.

Bibliography

1. Hotamisligil GS, Erbay E: **Nutrient sensing and inflammation in metabolic diseases**. *Nature reviews Immunology* 2008, **8**(12):923-934.
2. **Insulin signaling pathway- Homo Sapiens (human)** [http://www.genome.jp/kegg-bin/show_pathway?hsa04910]
3. Arbo I, Halle C, Malik D, Brattbakk HR, Johansen B: **Insulin induces fatty acid desaturase expression in human monocytes**. *Scand J Clin Lab Invest* 2011, **71**(4):330-339.
4. Mughal RS, Scragg JL, Lister P, Warburton P, Riches K, O'Regan DJ, Ball SG, Turner NA, Porter KE: **Cellular mechanisms by which proinsulin C-peptide prevents insulin-induced neointima formation in human saphenous vein**. *Diab tologia* 2010, **53**(8):1761-1771.
5. Saltiel AR, Kahn CR: **Insulin signalling and the regulation of glucose and lipid metabolism**. *Nature* 2001, **414**(6865):799-806.
6. Schwartz MW, Seeley RJ, Tschop MH, Woods SC, Morton GJ, Myers MG, D'Alessio D: **Cooperation between brain and islet in glucose homeostasis and diabetes**. *Nature* 2013, **503**(7474):59-66.
7. Fantin VR, Wang Q, Lienhard GE, Keller SR: **Mice lacking insulin receptor substrate 4 exhibit mild defects in growth, reproduction, and glucose homeostasis**. *American journal of physiology Endocrinology and metabolism* 2000, **278**(1):E127-133.
8. Michael MD, Kulkarni RN, Postic C, Previs SF, Shulman GI, Magnuson MA, Kahn CR: **Loss of insulin signaling in hepatocytes leads to severe insulin resistance and progressive hepatic dysfunction**. *Mol Cell* 2000, **6**(1):87-97.
9. DeFronzo RA, Tripathy D: **Skeletal muscle insulin resistance is the primary defect in type 2 diabetes**. *Diabetes Care* 2009, **32 Suppl 2**:S157-163.
10. Greenfield MS, Doberne L, Kraemer F, Tobey T, Reaven G: **Assessment of insulin resistance with the insulin suppression test and the euglycemic clamp**. *Diabetes* 1981, **30**(5):387-392.
11. DeFronzo R, Deibert D, Hendler R, Felig P, Soman V: **Insulin sensitivity and insulin binding to monocytes in maturity-onset diabetes**. *J Clin Invest* 1979, **63**(5):939-946.
12. Storlien LH, Higgins JA, Thomas TC, Brown MA, Wang HQ, Huang XF, Else PL: **Diet composition and insulin action in animal models**. *Br J Nutr* 2000, **83 Suppl 1**:S85-90.

13. Stout RW: **Hyperinsulinemia and atherosclerosis**. *Diabetes* 1996, **45 Suppl 3**:S45-46.
14. Yip J, Facchini FS, Reaven GM: **Resistance to insulin-mediated glucose disposal as a predictor of cardiovascular disease**. *J Clin Endocrinol Metab* 1998, **83**(8):2773-2776.
15. Fernandez-Real JM, Ricart W: **Insulin resistance and chronic cardiovascular inflammatory syndrome**. *Endocr Rev* 2003, **24**(3):278-301.
16. Cross DA, Alessi DR, Cohen P, Andjelkovich M, Hemmings BA: **Inhibition of glycogen synthase kinase-3 by insulin mediated by protein kinase B**. *Nature* 1995, **378**(6559):785-789.
17. Cusi K, Maezono K, Osman A, Pendergrass M, Patti ME, Pratipanawatr T, DeFronzo RA, Kahn CR, Mandarino LJ: **Insulin resistance differentially affects the PI 3-kinase- and MAP kinase-mediated signaling in human muscle**. *J Clin Invest* 2000, **105**(3):311-320.
18. Shepherd PR, Nave BT, Siddle K: **Insulin stimulation of glycogen synthesis and glycogen synthase activity is blocked by wortmannin and rapamycin in 3T3-L1 adipocytes: evidence for the involvement of phosphoinositide 3-kinase and p70 ribosomal protein-S6 kinase**. *Biochem J* 1995, **305 (Pt 1)**:25-28.
19. Isenovic ER, Fretaud M, Dobutovic B, Sudar E, Smiljanic K, Zaric B, Trpkovic A, Marche P: **A novel hypothesis regarding the possible involvement of cytosolic phospholipase 2 in insulin-stimulated proliferation of vascular smooth muscle cells**. *Cell Biol Int* 2009, **33**(3):386-392.
20. Mittelman SD, Fu YY, Rebrin K, Steil G, Bergman RN: **Indirect effect of insulin to suppress endogenous glucose production is dominant, even with hyperglucagonemia**. *J Clin Invest* 1997, **100**(12):3121-3130.
21. Anderson KM, Roshak A, Winkler JD, McCord M, Marshall LA: **Cytosolic 85-kDa phospholipase A2-mediated release of arachidonic acid is critical for proliferation of vascular smooth muscle cells**. *J Biol Chem* 1997, **272**(48):30504-30511.
22. Fernandez Mejia C: **Molecular Basis of Type 2 Diabetes**. *Mol Endo* 2006, **87**:87.
23. Cersosimo E, Xu X, Musi N: **Potential role of insulin signaling on vascular smooth muscle cell migration, proliferation, and inflammation pathways**. *American journal of physiology Cell physiology* 2012, **302**(4):C652-657.
24. Montagnani M, Golovchenko I, Kim I, Koh GY, Goalstone ML, Mundhekar AN, Johansen M, Kucik DF, Quon MJ, Draznin B: **Inhibition of phosphatidylinositol 3-kinase enhances mitogenic actions of insulin in endothelial cells**. *J Biol Chem* 2002, **277**(3):1794-1799.

25. Geissmann F, Manz MG, Jung S, Sieweke MH, Merad M, Ley K: **Development of monocytes, macrophages, and dendritic cells**. *Science* 2010, **327**(5966):656-661.
26. Schipper HS, Nuboer R, Prop S, van den Ham HJ, de Boer FK, Kesmir C, Mombers IM, van Bekkum KA, Woudstra J, Kieft JH *et al*: **Systemic inflammation in childhood obesity: circulating inflammatory mediators and activated CD14++ monocytes**. *Diab tologia* 2012, **55**(10):2800-2810.
27. Swirski FK, Nahrendorf M, Etzrodt M, Wildgruber M, Cortez-Retamozo V, Panizzi P, Figueiredo JL, Kohler RH, Chudnovskiy A, Waterman P *et al*: **Identification of splenic reservoir monocytes and their deployment to inflammatory sites**. *Science* 2009, **325**(5940):612-616.
28. Ziegler-Heitbrock L, Ancuta P, Crowe S, Dalod M, Grau V, Hart DN, Leenen PJ, Liu YJ, MacPherson G, Randolph GJ *et al*: **Nomenclature of monocytes and dendritic cells in blood**. *Blood* 2010, **116**(16):e74-80.
29. Ziegler-Heitbrock L: **The CD14+ CD16+ blood monocytes: their role in infection and inflammation**. *J Leukoc Biol* 2007, **81**(3):584-592.
30. Schmidl C, Renner K, Peter K, Eder R, Lassmann T, Balwierz PJ, Itoh M, Nagao-Sato S, Kawaji H, Carninci P *et al*: **Transcription and enhancer profiling in human monocyte subsets**. *Blood* 2014, **123**(17):E90-E99.
31. Antal-Szalmas P, Strijp JA, Weersink AJ, Verhoef J, Van Kessel KP: **Quantitation of surface CD14 on human monocytes and neutrophils**. *J Leukoc Biol* 1997, **61**(6):721-728.
32. Fleit HB, Kobasiuk CD: **THE HUMAN MONOCYTE-LIKE CELL-LINE THP-1 EXPRESSES FC-GAMMA-RI AND FC-GAMMA-RII**. *J Leukoc Biol* 1991, **49**(6):556-565.
33. Antal-Szalmas P, Strijp J, Weersink A, Verhoef J, Van Kessel K: **Quantitation of surface CD14 on human monocytes and neutrophils**. *J Leukoc Biol* 1997, **61**(6):721-728.
34. Tobias PS, Soldau K, Kline L, Lee JD, Kato K, Martin TP, Ulevitch RJ: **Cross-linking of lipopolysaccharide (LPS) to CD14 on THP-1 cells mediated by LPS-binding protein**. *J Immunol* 1993, **150**(7):3011-3021.
35. Kirkland TN, Finley F, Leturcq D, Moriarty A, Lee JD, Ulevitch RJ, Tobias PS: **Analysis of lipopolysaccharide binding by CD14**. *J Biol Chem* 1993, **268**(33):24818-24823.
36. Motton DD, Keim NL, Tenorio FA, Horn WF, Rutledge JC: **Postprandial monocyte activation in response to meals with high and low glycemic loads in overweight women**. *Am J Clin Nutr* 2007, **85**(1):60-65.
37. Oestvang J, Johansen B: **PhospholipaseA2: a key regulator of inflammatory signalling and a connector to fibrosis development in atherosclerosis**. *Biochim Biophys Acta* 2006, **1761**(11):1309-1316.

38. Klop B, van de Geijn GJ, Njo TL, Janssen HW, Rietveld AP, van Miltenburg A, Fernandez-Sender L, Elte JW, Castro Cabezas M: **Leukocyte cell population data (volume conductivity scatter) in postprandial leukocyte activation**. *International journal of laboratory hematology* 2013, **35**(6):644-651.
39. Jostarndt K, Gellert N, Rubic T, Weber C, Kuhn H, Johansen B, Hrboticky N, Neuzil J: **Dissociation of apoptosis induction and CD36 upregulation by enzymatically modified low-density lipoprotein in monocytic cells**. *Biochem Biophys Res Commun* 2002, **290**(3):988-993.
40. Auwerx J: **The human leukemia cell line, THP-1: a multifacetted model for the study of monocyte-macrophage differentiation**. *Experientia* 1991, **47**(1):22-31.
41. Takashiba S, Van Dyke TE, Amar S, Murayama Y, Soskolne AW, Shapira L: **Differentiation of monocytes to macrophages primes cells for lipopolysaccharide stimulation via accumulation of cytoplasmic nuclear factor κB**. *Infect Immun* 1999, **67**(11):5573-5578.
42. Stoppelli MP, Corti A, Soffientini A, Cassani G, Blasi F, Assoian RK: **Differentiation-enhanced binding of the amino-terminal fragment of human urokinase plasminogen activator to a specific receptor on U937 monocytes**. *Proceedings of the National Academy of Sciences* 1985, **82**(15):4939-4943.
43. Tsuchiya S, Yamabe M, Yamaguchi Y, Kobayashi Y, Konno T, Tada K: **Establishment and characterization of a human acute monocytic leukemia cell line (THP-1)**. *Int J Cancer* 1980, **26**(2):171-176.
44. Adams DO, Hamilton TA: **The cell biology of macrophage activation**. *Annu Rev Immunol* 1984, **2**:283-318.
45. Altieri DC, Edgington TS: **Sequential receptor cascade for coagulation proteins on monocytes. Constitutive biosynthesis and functional prothrombinase activity of a membrane form of factor V/Va**. *J Biol Chem* 1989, **264**(5):2969-2972.
46. Gao D, Trayhurn P, Bing C: **1,25-Dihydroxyvitamin D3 inhibits the cytokine-induced secretion of MCP-1 and reduces monocyte recruitment by human preadipocytes**. *International journal of obesity (2005)* 2013, **37**(3):357-365.
47. Qin Z: **The use of THP-1 cells as a model for mimicking the function and regulation of monocytes and macrophages in the vasculature**. *Atherosclerosis* 2012, **221**(1):2-11.
48. H. Lodish AB, P. Matsudaira, C. A. Kaiser, M. Krieger, M. P. Scott, S. L. Zipursky,, and J. Darnell: **Molecular Cell Biology**, vol. 5; 2004.
49. Alberts B: **Molecular Biology of the Cell**: Garland Science; 2008.
50. Freshney RI: **Culture of animal cells: a manual of basic technique and specialized applications**. Hoboken, N. J.: Wiley-Blackwell; 2011.

51. Gustincich S, Schneider C: **Serum deprivation response gene is induced by serum starvation but not by contact inhibition**. *Cell Growth Differ* 1993, **4**(9):753-760.
52. Ludwig DDS: **The glycemic index - Physiological mechanisms relating to obesity, diabetes, and cardiovascular disease**. *JAMA-J Am Med Assoc* 2002, **287**(18):2414-2423.
53. Kappert K, Meyborg H, Clemenz M, Graf K, Fleck E, Kintscher U, Stawowy P: **Insulin facilitates monocyte migration: a possible link to tissue inflammation in insulin-resistance**. *Biochem Biophys Res Commun* 2008, **365**(3):503-508.
54. Kelly T, Yang W, Chen CS, Reynolds K, He J: **Global burden of obesity in 2005 and projections to 2030**. *International journal of obesity (2005)* 2008, **32**(9):1431-1437.
55. Ouchi N, Parker JL, Lugus JJ, Walsh K: **Adipokines in inflammation and metabolic disease**. *Nature reviews Immunology* 2011, **11**(2):85-97.
56. Sartipy P, Loskutoff DJ: **Monocyte chemoattractant protein 1 in obesity and insulin resistance**. *Proc Natl Acad Sci U S A* 2003, **100**(12):7265-7270.
57. Spite M, Hellmann J, Tang Y, Mathis SP, Kosuri M, Bhatnagar A, Jala VR, Haribabu B: **Deficiency of the leukotriene B4 receptor, BLT-1, protects against systemic insulin resistance in diet-induced obesity**. *J Immunol* 2011, **187**(4):1942-1949.
58. Gogg S, Smith U, Jansson P-A: **Increased MAPK Activation and Impaired Insulin Signaling in Subcutaneous Microvascular Endothelial Cells in Type 2 Diabetes: The Role of Endothelin-1**. *Diabetes* 2009, **58**(10):2238-2245.
59. Wunderlich FT, Strohle P, Konner AC, Gruber S, Tovar S, Bronneke HS, Juntti-Berggren L, Li LS, van Rooijen N, Libert C *et al*: **Interleukin-6 signaling in liver-parenchymal cells suppresses hepatic inflammation and improves systemic insulin action**. *Cell metabolism* 2010, **12**(3):237-249.
60. Stokes RW, Doxsee D: **The receptor-mediated uptake, survival, replication, and drug sensitivity of Mycobacterium tuberculosis within the macrophage-like cell line THP-1: a comparison with human monocyte-derived macrophages**. *Cell Immunol* 1999, **197**(1):1-9.
61. **MAINTENANCE & CULTURE OF THP-1 CELLS** [http://www.bowdish.ca/lab/wp-content/uploads/2011/07/THP-1-propagation-culture.pdf]
62. Ricardo R, Phelan K: **Counting and determining the viability of cultured cells**. *Journal of visualized experiments : JoVE* 2008(16).
63. Gunetti M, Castiglia S, Rustichelli D, Mareschi K, Sanavio F, Muraro M, Signorino E, Castello L, Ferrero I, Fagioli F: **Validation of analytical**

methods in GMP: the disposable Fast Read 102(R) device, an alternative practical approach for cell counting. *Journal of translational medicine* 2012, **10**:112.
64. Wigg AJ, Phillips JW, Wheatland L, Berry MN: **Assessment of cell concentration and viability of isolated hepatocytes using flow cytometry**. *Anal Biochem* 2003, **317**(1):19-25.
65. Rotoli BM, Guidi P, Bonelli B, Bernardeschi M, Bianchi MG, Esposito S, Frenzilli G, Lucchesi P, Nigro M, Scarcelli V *et al*: **Imogolite: an aluminosilicate nanotube endowed with low cytotoxicity and genotoxicity**. *Chem Res Toxicol* 2014, **27**(7):1142-1154.
66. Sykes ML, Avery VM: **Development of an Alamar Blue viability assay in 384-well format for high throughput whole cell screening of Trypanosoma brucei brucei bloodstream form strain 427**. *Am J Trop Med Hyg* 2009, **81**(4):665-674.
67. Celis JE: **Cell biology**: Elsevier; 2006.
68. O'Brien J, Wilson I, Orton T, Pognan F: **Investigation of the Alamar Blue (resazurin) fluorescent dye for the assessment of mammalian cell cytotoxicity**. *Eur J Biochem* 2000, **267**(17):5421-5426.
69. **Product datasheet** [http://www.rndsystems.com/Products/ar002]
70. Rampersad SN: **Multiple applications of Alamar Blue as an indicator of metabolic function and cellular health in cell viability bioassays**. *Sensors (Basel, Switzerland)* 2012, **12**(9):12347-12360.
71. Maddigan A, Truitt L, Arsenault R, Freywald T, Allonby O, Dean J, Narendran A, Xiang J, Weng A, Napper S *et al*: **EphB receptors trigger Akt activation and suppress Fas receptor-induced apoptosis in malignant T lymphocytes**. *J Immunol* 2011, **187**(11):5983-5994.
72. Lyons AB: **Analysing cell division in vivo and in vitro using flow cytometric measurement of CFSE dye dilution**. *J Immunol Methods* 2000, **243**(1-2):147-154.
73. Camplejohn RS: **Flow Cytometric Measurement of Cell Proliferation**. In., vol. 57; 2001: 133-143.
74. **Introduction to Flow Cytometry** [http://www.bio.umass.edu/micro/immunology/facs542/facsprin.htm]
75. Van Vre EA, Bult H, Hoymans VY, Van Tendeloo VFI, Vrints CJ, Bosmans JM: **Human C-reactive protein activates monocyte-derived dendritic cells and induces dendritic cell-mediated T-cell activation**. *Arteriosclerosis Thrombosis and Vascular Biology* 2008, **28**(3):511-518.
76. Go Y-M, Jones DP: **Cysteine/cystine redox signaling in cardiovascular disease**. *Free Radic Biol Med* 2011, **50**(4):495-509.
77. Feuerherm AJ, Jorgensen KM, Sommerfelt RM, Eidem LE, Laegreid A, Johansen B: **Platelet-activating factor induces proliferation in differentiated keratinocytes**. *Mol Cell Biochem* 2013, **384**(1-2):83-94.

78. Qin J, Yang X, Mi J, Wang J, Hou J, Shen T, Li Y, Wang B, Li X, Zhu W: **Enhanced antidepressant-like effects of the macromolecule trefoil factor 3 by loading into negatively charged liposomes**. *International journal of nanomedicine* 2014, **9**:5247-5257.
79. Dimitriadis G, Maratou E, Boutati E, Psarra K, Papasteriades C, Raptis SA: **Evaluation of glucose transport and its regulation by insulin in human monocytes using flow cytometry**. *Cytometry Part A : the journal of the International Society for Analytical Cytology* 2005, **64**(1):27-33.
80. Iida KT, Suzuki H, Sone H, Shimano H, Toyoshima H, Yatoh S, Asano T, Okuda Y, Yamada N: **Insulin inhibits apoptosis of macrophage cell line, THP-1 cells, via phosphatidylinositol-3-kinase-dependent pathway**. *Arterioscler Thromb Vasc Biol* 2002, **22**(3):380-386.
81. Johansen A: **Characterization of Cellular Effects of Insulin in SW982 Fibroblast-like Synoviocytes**. 2014.
82. Franke TF, Kaplan DR, Cantley LC: **PI3K: downstream AKTion blocks apoptosis**. *Cell* 1997, **88**(4):435-437.
83. Zhang Q, Liu SH, Erikson M, Lewis M, Unemori E: **Relaxin activates the MAP kinase pathway in human endometrial stromal cells**. *J Cell Biochem* 2002, **85**(3):536-544.
84. Leffler M, Hrach T, Stuerzl M, Horch RE, Herndon DN, Jeschke MG: **Insulin attenuates apoptosis and exerts anti-inflammatory effects in endotoxemic human macrophages**. *J Surg Res* 2007, **143**(2):398-406.
85. Fischoeder A, Meyborg H, Stibenz D, Fleck E, Graf K, Stawowy P: **Insulin augments matrix metalloproteinase-9 expression in monocytes**. *Cardiovasc Res* 2007, **73**(4):841-848.
86. Staiger K, Staiger H, Schweitzer MA, Metzinger E, Balletshofer B, Haring HU, Kellerer M: **Insulin and its analogue glargine do not affect viability and proliferation of human coronary artery endothelial and smooth muscle cells**. *Diab tologia* 2005, **48**(9):1898-1905.
87. Li GL, Barrett EJ, Wang H, Chai WD, Liu ZQ: **Insulin at physiological concentrations selectively activates insulin but not insulin-like growth factor I (IGF-I) or insulin/IGF-I hybrid receptors in endothelial cells**. *Endocrinology* 2005, **146**(11):4690-4696.
88. Despres JP, Lamarche B, Mauriege P, Cantin B, Lupien PJ, Dagenais GR: **Risk factors for ischaemic heart disease: is it time to measure insulin?** *Eur Heart J* 1996, **17**(10):1453-1454.
89. Liu P, Cheng H, Roberts TM, Zhao JJ: **Targeting the phosphoinositide 3-kinase pathway in cancer**. *Nature reviews Drug discovery* 2009, **8**(8):627-644.
90. Wong K-K, Engelman JA, Cantley LC: **Targeting the PI3K signaling pathway in cancer**. *Curr Opin Genet Dev* 2010, **20**(1):87-90.

91. Weichhaus M, Broom J, Wahle K, Bermano G: **A novel role for insulin resistance in the connection between obesity and postmenopausal breast cancer**. *Int J Oncol* 2012, **41**(2):745-752.
92. Mu N, Zhu Y, Wang Y, Zhang H, Xue F: **Insulin resistance: a significant risk factor of endometrial cancer**. *Gynecol Oncol* 2012, **125**(3):751-757.
93. Godsland IF: **Insulin resistance and hyperinsulinaemia in the development and progression of cancer**. *Clinical science (London, England : 1979)* 2010, **118**(5):315-332.
94. Hursting SD, Dunlap SM: **Obesity, metabolic dysregulation, and cancer: a growing concern and an inflammatory (and microenvironmental) issue**. *Ann N Y Acad Sci* 2012, **1271**:82-87.
95. Motani A, Forster L, Tull S, Anggard EE, Ferns GA: **Insulin-like growth factor-I modulates monocyte adhesion to EAhy 926 endothelial cells**. *Int J Exp Pathol* 1996, **77**(1):31-35.
96. Ding XZ, Fehsenfeld DM, Murphy LO, Permert J, Adrian TE: **Physiological concentrations of insulin augment pancreatic cancer cell proliferation and glucose utilization by activating MAP kinase, PI3 kinase and enhancing GLUT-1 expression**. *Pancreas* 2000, **21**(3):310-320.
97. Mograbi B, Rochet N, Emiliozzi C, Rossi B: **Adhesion of human monocytic THP-1 cells to endothelial cell adhesion molecules or extracellular matrix proteins via beta(1) integrins regulates heparin binding epidermal growth factor-like growth factor (HB-EGF) expression**. *Eur Cytokine Netw* 1999, **10**(1):79-86.
98. Hamid R, Rotshteyn Y, Rabadi L, Parikh R, Bullock P: **Comparison of alamar blue and MTT assays for high through-put screening**. *Toxicology in vitro : an international journal published in association with BIBRA* 2004, **18**(5):703-710.

Appendix

A. All biological replicas (n = 5) for the representative experiment in figure 7.

Table A.1 The data represent mean ± SD where Ctrl is set to 100 % proliferation. * p = 0.01 - 0.05, ** p = 0.001 - 0.01, *** p < 0.001 versus untreated cells (Ctrl).

Treatment	24 h	48 h	72 h
20 nM INS	107	100	96
± SD	8	11	9
100 nM INS	123*	104	94
± SD	12	13	1
1 µM INS	113	111	92
± SD	6	10	5
FBS 10 %	136**	145**	171***
± SD	12	5	9

B. All biological replicas (n = 3) for the representative experiment in figure 9.

Table B.1 The data indicate resazurin metabolization as mean ± SD where Ctrl is set to 100 % metabolic activity. The different number of cells seeded, and the cell metabolic activity was measured following 24 h of insulin treatment (1 µM) and 1, 2, 3 and 4 h of resazurin metabolization, respectively. *** $p < 0.001$ versus untreated cells (Ctrl).

Number of Cells Seeded	1 h	2 h	3 h	4 h
5000	100	100	100	100
± SD	2	3	3	4
10000	102	101	101	100
± SD	6	3	3	3
20000	105***	105***	108***	109***
± SD	3	3	3	3

C. All biological replicas (For 8 h (n = 3), for 16 and 36 h (n = 4), for 24 h (for Ctrl and 1 μM INS, n = 7. For FBS 2%, 20 nM INS and 100 nM INS, n = 4) for the representative experiment in figure 10.

Table C.1 The data represent resazurin metabolization as mean ± SD where Ctrl is set to 100 % metabolic activity. ** p = 0.001 - 0.01 versus untreated cells (Ctrl) and 1 μM INS-treated cells.

Treatment	8 h	16 h	24 h	36 h
20 nM INS	100	101	105**	100
± SD	9	8	5	4
100 nM INS	100	101	105**	99
± SD	8	6	4	5
1 μM INS	99	99	101	99
± SD	8	8	6	4
FBS 2 %	104	106	109**	101
± SD	14	11	10	10